

UC Merced

UC Merced Previously Published Works

Title

Visualizing in situ translational activity for identifying and sorting slow-growing archaeal–bacterial consortia

Permalink

<https://escholarship.org/uc/item/0283n05z>

Journal

Proceedings of the National Academy of Sciences of the United States of America, 113(28)

ISSN

0027-8424

Authors

Hatzenpichler, Roland
Connon, Stephanie A
Goudeau, Danielle
[et al.](#)

Publication Date

2016-07-12

DOI

10.1073/pnas.1603757113

Peer reviewed

1 **Visualizing *in situ* translational activity for identifying and sorting slow-**
2 **growing archaeal-bacterial consortia**

3
4 Roland Hatzenpichler^{a,1}, Stephanie A. Connon^a, Danielle Goudeau^b, Rex R. Malmstrom^b, Tanja
5 Woyke^b, Victoria J. Orphan^{a,1}

6
7 ^a Division of Geological and Planetary Sciences, California Institute of Technology, Pasadena,
8 CA-91125, USA

9 ^b Department of Energy Joint Genome Institute, Walnut Creek, CA-94598, USA

10 ¹ Address correspondence to hatzenpichler@caltech.edu and vorphan@gps.caltech.edu

11
12 **Short title:** Identifying and sorting active microbial consortia

13
14 **Keywords:** activity-based cell-sorting, BONCAT, click chemistry, ecophysiology, single cell
15 microbiology

16
17 **Author contributions:** R.H. and V.J.O. designed research; R.H., S.A.C, and D.G. performed
18 research; R.M., T.W., and V.J.O. contributed new reagents/analytic tools; R.H. and V.J.O.
19 analyzed data; R.H. and V.J.O. wrote the paper with inputs from all authors.

20
21 **Classification:** Biological Sciences, Microbiology

25 **Abstract**

26 In order to understand the biogeochemical roles of microorganisms in the environment, it is
27 important to determine when and under which conditions they are metabolically active.
28 Bioorthogonal non-canonical amino acid tagging (BONCAT) can reveal active cells by tracking
29 the incorporation of synthetic amino acids into newly synthesized proteins. The phylogenetic
30 identity of translationally active cells can be determined by combining BONCAT with rRNA-
31 targeted fluorescence *in situ* hybridization (BONCAT-FISH). In theory, BONCAT-labeled cells
32 could be isolated with fluorescence-activated cell-sorting (BONCAT-FACS) for subsequent
33 genetic analyses. Here, in the first application of BONCAT-FISH and BONCAT-FACS within
34 an environmental context, we probe the translational activity of microbial consortia catalyzing
35 the anaerobic oxidation of methane (AOM), a dominant sink of methane in the ocean. These
36 consortia, which typically are composed of anaerobic methane-oxidizing archaea (ANME) and
37 sulfate-reducing bacteria, have been difficult to study due to their slow *in situ* growth rates, and
38 fundamental questions remain about their ecology and diversity of interactions occurring
39 between ANME and associated partners. Our activity-correlated analyses of >16,400 microbial
40 aggregates provide the first evidence that AOM-consortia affiliated with all five major ANME-
41 clades are concurrently active under controlled conditions. Surprisingly, sorting of individual
42 BONCAT-labeled consortia followed by whole genome amplification and 16S rRNA gene
43 sequencing revealed previously unrecognized interactions of ANME with members of the poorly
44 understood phylum *Verrucomicrobia*. This finding, together with our observation that ANME-
45 associated *Verrucomicrobia* are found in a variety of geographically distinct methane seep
46 environments, suggests a broader range of symbiotic relationships within AOM-consortia than
47 previously thought.

48

49 **Significance statement**

50 One of the biggest challenges in environmental microbiology is to determine the activity of
51 uncultured cells directly in their habitat. We report on the application of bioorthogonal non-
52 canonical amino acid tagging (BONCAT), a high-throughput approach to detecting protein
53 synthesis in individual cells by fluorescence staining on deep-sea methane seep sediments. By
54 combining BONCAT with fluorescence *in situ* hybridization (FISH), we visualized active
55 archaeal-bacterial consortia catalyzing the anaerobic oxidation of methane. We further developed
56 a novel approach that combines BONCAT with fluorescence-activated cell-sorting (FACS) to
57 separate translationally active cells from complex samples. BONCAT-FACS enabled us to
58 directly link the identities of anaerobic methane-oxidizing archaea with their partner bacteria for
59 individual active consortia, uncovering previously unknown interactions between these archaea
60 and *Verrucomicrobia*.

61

62 \body

63 **Introduction**

64 Some of the most important goals of environmental microbiology are to understand the
65 physiology, niche differentiation, and activities of microorganisms in the context of their habitat.
66 Studies focusing on the mere presence of a cell or gene in a sample can only provide limited
67 information about the metabolic capabilities of an organism. Coupling the identification of an
68 uncultured microbe with its *in situ* activity thus has been referred to as the “Holy Grail” of
69 microbial ecology (1). While bulk techniques, such as meta-transcriptomics and meta-proteomics
70 or stable isotope probing targeted at DNA, RNA, or proteins, have provided us with exciting new
71 insights into microbial ecophysiology (1-3), they cannot resolve cellular activities on the micron
72 scale. The combination of rRNA-targeted fluorescence *in situ* hybridization (FISH) with single-
73 cell resolving stable isotope analysis offers a direct, targeted approach for detailed investigations
74 of microbial structure-function relationships (4, 5).

75 Single cell methods for direct assessment of metabolic activity include three broadly
76 applicable approaches were available for studying the *in situ* anabolic activity of individual cells:
77 micro-autoradiography (MAR; 6), secondary ion mass spectroscopy (SIMS and nanoSIMS; 7),
78 and Raman microspectroscopy (Raman; 8). Each of these techniques have technical challenges
79 or limited instrument availability which have slowed their wide adoption in the field (1, 5, 9).
80 MAR and SIMS are also destructive methods that cannot be combined with downstream analysis
81 such as cell-sorting, sub-culturing, or genomic sequencing. Another problem is that many
82 biomolecules are prohibitively expensive or even unavailable in their isotopically labeled form.
83 A universally applicable approach that circumvents these limitations was recently established by
84 combining the general labeling of active cells via heavy water (D₂O) with their subsequent
85 identification via FISH and sorting via Raman-coupled optical tweezers (10). Complementary to
86 detecting anabolic activity via isotope labeling, a fluorescence technique based on the
87 visualization of bacterial reductase activity via redox sensing (Redox sensor green) has also been
88 described (11, 12). The general applicability and exact mechanism of this proprietary staining
89 method are, however, unknown.

90 An alternative approach for studying microbial ecophysiology that does not depend on
91 isotopes is labeling active cells via chemically modifiable analogs of biomolecules (9, 13, 14).
92 Bioorthogonal non-canonical amino acid tagging (BONCAT) is a non-destructive technique first
93 applied in neurobiology (15, 16). Last year, BONCAT was adapted for the study of uncultured
94 archaea and bacteria within environmental samples (9, 14). BONCAT depends on the addition of
95 a bioorthogonal (*i.e.* non-interacting with cellular functionalities) synthetic (non-canonical)
96 amino acid to a sample. After its uptake (the exact process is currently unknown), the amino acid
97 is able to exploit the substrate promiscuity of specific amino acyl-tRNA synthetases, the
98 enzymes catalyzing the esterification of amino acids with their respective cognate tRNAs, to get
99 incorporated into *de novo* peptides (17). Protein synthesis-active cells can in the following be
100 visualized via a highly selective click chemistry-mediated labeling reaction that conjugates a
101 modified fluorescence dye to a chemical reporter group (an azide or alkyne) of the bioorthogonal

102 amino acid (Fig. 1A). While a wide range of synthetic amino acids exists, only a small number
103 are able to exploit the natural translational machinery without the need for genetic modification
104 of the cell (18). To date, the *L*-methionine (Met) surrogates *L*-azidohomoalanine (AHA) and *L*-
105 homopropargylglycine (HPG) (17) have found the widest application (e.g. 16, 19, 20-24). In a
106 proof-of-principle investigation, BONCAT was applied to environmental samples and found to
107 be generally applicable to uncultured archaea and bacteria (9, 14). BONCAT has been
108 demonstrated to correlate well with other, independent proxies of cellular growth, *i.e.* the
109 incorporation of isotopically labeled compounds as detected by nanoscale SIMS ($^{15}\text{NH}_4^+$; 9)
110 and MAR (^{35}S -Met; 14). In addition, a protocol for the concomitant taxonomic identification of
111 translationally active cells via rRNA-targeted FISH (*i.e.* BONCAT-FISH), was recently
112 developed (9; Fig. 1A,B).

113 In this study, we applied HPG to deep-sea methane seep sediments in which the sulfate-
114 coupled anaerobic oxidation of methane (AOM) is occurring. AOM accounts for the removal of
115 ~80% of the CH_4 released from ocean sediments ($>400 \text{ Gt year}^{-1}$) and is a key process in the
116 biogeochemical cycling of this highly potent greenhouse gas (25). In marine seeps AOM is
117 predominantly catalyzed by a symbiosis of anaerobic methane-oxidizing euryarchaeotes
118 (ANME) with sulfate-reducing bacteria (SRB), which form consortia of varying cell number
119 (~ 10 to $\sim 10^5$ cells) and morphology (7, 26). Their syntrophic partnership is hypothesized to be
120 mediated by direct electron transfer (27, 28; Scheller et al., in revision) and/or diffusible
121 intermediates (29, 30).

122 Several different ANME-clades (referred to as ANME-1a, -1b, -2a, 2b, 2c, and -3) have been
123 observed to aggregate with different representatives of SRB (particularly members of the
124 *Desulfosarcina*, *Desulfococcus*, and *Desulfobulbus* genera), with multiple ANME-SRB consortia
125 of different taxonomies commonly co-existing in seep sediments without apparent competitive
126 exclusion of one another. The potential for ecological niche partitioning within these highly
127 diverse, yet seemingly functionally redundant associations is not well understood. Previously, it
128 was demonstrated that temperature (31), CH_4 partial pressure (31), concentrations of sulfate (32,
129 33) and sulfide (33), as well as the availability of nitrogen (34, 35) may influence distribution
130 and activity of AOM-consortia. In addition, ANME-community structure can vary dramatically
131 between geographically proximate sites as well as distinct sediment layers (36, 37). Whether
132 different ANME-subgroups in a given sample show variable activities depending on specific
133 physico-chemical or ecological conditions or are all metabolically active at a given time is
134 unknown. In addition to sulfate reducers, other bacterial lineages, including members of the
135 alpha-, beta-, gamma-, and epsilon-proteobacteria, have been observed to form physical
136 associations with ANME (38; Trembath-Reichert et al., in prep.). The metabolic interactions
137 underlying these relationships are, however, yet to be determined.

138 Our study represents the first research application of BONCAT-FISH in environmental
139 microbiology. We tested the influence of methane on the metabolic activity (protein synthesis) of
140 diverse AOM-consortia in three sediment samples from two geographically and geochemically
141 distinct locations. We further developed a novel approach for isolating protein-synthesizing cells

142 identified using BONCAT via fluorescence-activated cell-sorting (FACS). Subsequent 16S
143 rRNA gene-based identification of individual AOM-consortia provided detailed aggregate-
144 specific information into specific archaeal-bacterial partnerships. This approach revealed
145 previously unrecognized metabolically active associations between ANME and new bacterial
146 groups outside the deltaproteobacteria.
147

148 **Results and Discussion**

149 **Establishment of HPG incubation experiments with methane seep sediment.** Samples
150 were obtained from a methane seep from Hydrate Ridge, Oregon, (sample #3730), and a seep
151 site in the Santa Monica basin, California, (samples #7135, 7136-37, and 7142). Anoxic
152 sediment microcosms were set up in the presence or absence of HPG (5 or 50 μM) and over-
153 pressurized (2 bars) with either N_2 or CH_4 followed by incubation in the dark at 4°C for 114
154 (#3730), 171 (#7135), 31 (#7136-37), and 25 (#7142) days. These long incubation times were
155 necessary due to the slow growth of ANME-SRB consortia (3-7 months; e.g. 39, 40, 41), which
156 is attributed to the very low free energy yield of sulfate-coupled AOM (40, 42). Subsampling for
157 molecular and geochemical analyses as well as exchange of gaseous headspace and seawater
158 were conducted at regular intervals. Details on incubation setup and sampling is provided in Tab.
159 S1.

160 **HPG amendment had no detectable effect on microbial community composition or**
161 **activity.** Adding a compound to an environmental sample always bears the risk of altering the
162 structure or function of the microbial community. Three independent lines of evidence suggest
163 that at the concentrations used in this study ($\leq 50 \mu\text{M}$), the methionine analog HPG did not affect
164 the geochemical activity or community structure of microbes within methane seep sediment for
165 up to 171 days of incubation. First, HPG addition had no effect on sulfide production, a reliable
166 proxy for sulfate-dependent AOM-activity (43) in time course experiments (up to 6 months). In
167 contrast, the removal of CH_4 led to a notable and expected decrease (Fig. S1A) in sulfide
168 production as previously reported (43; Fig. S1A). Second, seep sediment from Santa Monica
169 basin (sediment #7142) incubated with and without HPG over a period of 25 days showed
170 equivalent rates of AOM, as measured by ^{13}C -DIC production following $^{13}\text{CH}_4$ amendment (Fig.
171 S1B). Third, Illumina tag sequencing of the 16S rRNA V4 region of archaea and bacteria
172 revealed HPG additions had no statistically significant effect on sediment #3730 and #7135
173 community compositions (Fig. S2-4). More specifically, control incubations of #3730 are
174 indistinguishable from samples containing 50 μM HPG after 114 days of incubation (effect of
175 HPG, $p=0.20$), with an average Bray Curtis similarity of the communities of 94.4% between all
176 samples (Fig. S2-3). Sequences related to ANME-2c archaea make up a slightly higher
177 proportion in HPG-containing samples as compared to incubations without HPG, however this
178 observation was not statistically supported (Fig. S3 and S5). Similarly, for #7135, no differences
179 in the composition of the microbial community in general or ANME- and SRB-related lineages
180 in particular between samples incubated in the presence (5 or 50 μM) or absence of HPG were
181 observed (Fig. S2, S4, and S5). After 41 days, communities in incubations with or without HPG
182 were on average 92.1% similar (Bray Curtis; effect of HPG, $p=0.56$). This similarity decreased to
183 87.9-89.3% after an additional 130 days of incubation, but without a detectable effect from HPG
184 ($p=0.25$; Fig. S4A). The absence of CH_4 in the headspace, however, did result in a statistically
185 significant change in the microbial community ($p=0.042$; Fig. S2B).

186 These independent activity and community composition analyses all indicate that the
187 addition of the bioorthogonal amino acid HPG at concentrations up to 50 μM did not result in
188 any detectable changes in the seep microbial diversity or *in situ* activity up to 171 days.

189 **Fluorescence detection of translationally active cells.** To fluorescently label microbes
190 undergoing active protein synthesis during the incubation, a recently established BONCAT-
191 protocol based on the Cu(I)-catalyzed conjugation of HPG with an azide-dye (9, 14, 44) was
192 employed. In initial tests, no difference in fluorescence intensity or signal-to-noise ratio was
193 observed between ethanol-fixed, paraformaldehyde-fixed, or non-fixed AOM-consortia (data not
194 shown). All further experiments were thus performed on ethanol-fixed biomass, unless stated
195 otherwise. While several factors prohibit the absolute quantification of new proteins from
196 fluorescence data (discussed in the SI Appendix), semi-quantitative comparisons between
197 different cells of the same taxonomic group may offer information on the functional
198 (translational) activity of uncultured cells in the environment. Throughout the text, we refer to
199 DAPI-stained cell clusters that bound an ANME-specific (CARD)FISH-probe as “microbial
200 (AOM) consortia”. When cells within a DAPI-stained cluster could not be unambiguously
201 identified, we use the term “microbial aggregate” instead.

202 **BONCAT as a novel approach to study anabolic activity of AOM-consortia.** To establish
203 whether BONCAT can be used as a proxy for CH_4 -dependent translational activity of AOM-
204 consortia, we used sample #7136-37, representing the 9-15 cm depth horizon immediately
205 underlying sediment horizon #7135 (6-9 cm). After pre-incubation of the sediment in the absence
206 of CH_4 for 124 days, microcosm experiments were established with 50 μM HPG in the presence
207 or absence of CH_4 . After 31 days of incubation, microbial aggregates were extracted and
208 analyzed by microscopy ($n=1,554$). Under CH_4 -replete conditions, 24.9% of all microbial
209 aggregates were BONCAT-stained, while only 2.3% exhibited detectable translational activity
210 when CH_4 was absent from the headspace (Fig. 2). This initial test demonstrated that BONCAT
211 can be used to study the CH_4 -dependent anabolic activity of AOM-consortia.

212 **Sensitivity of BONCAT.** In all incubations, the relative abundance of translationally active
213 DAPI-stained microbial aggregates increased with time, with 65.8% and 48.5% of aggregates in
214 #3730 and #7135 showing a positive BONCAT signal at the end of incubation (114 and 171
215 days, respectively). It is interesting to note that already after 7 days of incubation, 5.6% of the
216 microbial aggregates in sediment #7135 were labeled by BONCAT (Fig. 2). Assuming that the
217 AOM-consortia studied here have growth rates comparable to those previously reported (2-7
218 months; 39, 40, 41), we estimate that BONCAT is able to detect the *in situ* activities of cells
219 within ANME-SRB consortia after 3.3-7.7% of their doubling time. Considering the differences
220 in the physiology of the organisms as well as the lower fluorescence signal-to-noise ratios
221 observed in environmental systems, this estimate is consistent with our finding of a BONCAT-
222 detection limit of $<2\%$ of generation time for slow-growing *E. coli* (9).

223 At this time, it is unclear why up to half of the DAPI-stained consortia were not BONCAT-
224 stained during the AOM incubation experiments. This may have been the result of storing these
225 deep-sea samples in the lab, variable amino acid uptake, or low levels of protein synthesis that

226 are below detection with BONCAT. The combined application of BONCAT and rRNA-targeted
227 FISH demonstrated that all ANME-lineages present in our samples are able to incorporate HPG
228 into their biomass (discussed below). This suggests that an inability to take up HPG into cells is
229 likely not a problem in our AOM microcosms. This idea is further supported by the observation
230 that AHA and HPG are taken up and incorporated by a range of bacterial and archaeal cultures,
231 including methanogens and sulfate reducers (9, 44).

232 **BONCAT-FISH as a tool for microbial *in situ* activity studies.** While the quantitative
233 isotopic analysis provided by secondary ion mass spectrometry (SIMS and nanoSIMS) is
234 currently unparalleled by other single cell techniques, the specialized instrumentation and cost
235 along with comparatively lower sample throughput have restricted its widespread application in
236 the field (10-100 consortia per study; e.g. 7, 27, 34, 35). Many fundamental questions in
237 microbial ecology regarding the activity and metabolic potential of environmental microbes *in*
238 *situ*, however, can be addressed with lower precision methods.

239 To demonstrate the utility of BONCAT as a comparatively higher throughput method for
240 tracking microbial biosynthetic activity, we used epifluorescence microscopy combined with
241 FISH-BONCAT to investigate the *in situ* translational activities of 16,438 individual microbial
242 aggregates in the presence or absence of CH₄. In total, 12,652 aggregates from four #3730
243 microcosms incubated for 30 and 114 days were analyzed. In addition, the activities of 2,232
244 aggregates from six incubations of sediment #7135 after 7, 41, and 171 days of incubation were
245 determined. To assess whether the activity of individual consortia is influenced by the
246 phylogenetic affiliation of their partners we combined BONCAT with rRNA-targeted FISH (Fig.
247 1B). Following our recently established protocol (9, 44), we used 11 different 16S and 23S
248 rRNA-targeted oligonucleotide probes labeled with either a fluorescence dye or horseradish
249 peroxidase (for catalyzed reporter deposition FISH, CARD-FISH) to target the different ANME-
250 populations and their associated bacteria present in our samples. These were applied in 11
251 different combinations (see SI Appendix and Tab. S2 and S3 for details) to study the activity of
252 AOM-consortia in the presence or absence of CH₄. In total, we visualized the translational
253 activities of 1,346 taxonomically identified AOM-consortia (representative images in Fig. 3;
254 results in Fig. 2, Tab. 1, Tab. S2).

255 **BONCAT-FISH reveals the co-occurrence of diverse and active AOM consortia.**
256 Domain-specific FISH-probes (Arch915 and EUB338mix) hybridized 37.6% (114 days) and
257 51.8% (41 days) of microbial aggregates in CH₄-containing incubations of sediment #3730 and
258 #7135, respectively. In contrast, the combined application of 5 fluorescently labeled
259 oligonucleotide probes specific for the main ANME-subpopulations present in our samples
260 (ANME-1, -2a, -2b, and -2c) yielded positive results for only 5.4% (#3730, 114 days) and 5.8%
261 (#7135, 41 days) of microbial aggregates in CH₄-containing samples. Two other groups of
262 ANME archaea, nitrate-dependent ANME-2d (45) as well as ANME-3 were absent from our
263 methane seep 16S rRNA iTAG datasets and thus were not probed by FISH. As compared to
264 FISH, CARD-FISH yielded slightly lower detection rates for probe Arch915, specific for domain
265 *Archaea* (55.7% in FISH vs. 53.2% for CARD-FISH for #3730, 114 days of incubation). Similar

266 results were obtained for the combined application of ANME-specific probes, which together
267 hybridized 4.2% of microbial aggregates (5.4% with FISH; Fig. 2 and Tab. 1). Comparable
268 hybridization efficiencies were found for samples that had been incubated in the absence of HPG
269 (data not shown). Independent CARD-FISH experiments (see Tab. 1 and SI Appendix),
270 corroborated these findings.

271 The stark discrepancy between domain- and subpopulation-specific probes might be
272 explained by a combination of factors. First, several available probes specific for different
273 ANME-clades are predicted to have low accessibilities to their rRNA-target sites (46) and thus
274 may exhibit low fluorescence signal-to-noise ratios. In addition, while most published ANME-
275 probes are predicted to comprehensively and specifically detect the diversity of sequences in
276 rRNA-databases, we do not know how well these probes cover the full diversity of ANME in the
277 environment. For one subpopulation, ANME-2b, which was represented by 18-20% of all
278 ANME-related tag-sequences in our sediments (Fig. S5), we tried to overcome this problem by
279 designing a new probe, ANME-2b-729. When tested *in silico* this probe binds to 93% of all
280 ANME-2b 16S rRNA sequences and has at least two mismatches to all non-ANME-2b-related
281 rRNA-sequences in public and in-house databases. We successfully applied this new probe to
282 our sediment samples (Fig. 3E-F) and the results are described in Tab. 1 and Tab. S2.
283 Alternatively, it is possible that a fraction of DAPI-stained aggregates contained archaea
284 unaffiliated to ANME. Similar to most other marine sediments (37), seep sediment #7135 from
285 Santa Monica Basin hosts a variety of archaea unrelated to ANME (9-17% of all iTAG
286 sequences in our dataset). The archaeal population in Hydrate Ridge sediment #3730, in contrast,
287 is dominated by ANME (93.2-97.7% of all archaeal i-tags). This makes it unlikely that archaea
288 unrelated to ANME constituted a substantial number of microbial consortia in #3730.
289 Furthermore, to our knowledge, no other sediment-dwelling archaea have previously been
290 reported to occur in multicellular associations with bacteria. Additional discussions on FISH
291 using ANME-specific probes can be found in the SI Appendix.

292 Of all consortia detectable with an ANME-specific FISH probe, 91.4% (sample #3730) and
293 81.8% (sample #7135), were also BONCAT-positive. In contrast, only 81.4% (#3730) and
294 58.3% (#7135) of all positively hybridized microbial aggregates (using either domain- or
295 ANME-specific FISH probes) could be detected via BONCAT (Fig. 2 and Tab. S2). This lends
296 support to the view that rRNA-targeted FISH is not always a reliable proxy for cellular activity.
297 Notably, there was no statistically supported relationship between BONCAT- and FISH-signal
298 intensities of individual cells within AOM-consortia (n=5 consortia, each composed of 50-200
299 cells; not shown).

300 **Multiple co-occurring ANME subgroups were active under identical incubation**
301 **conditions.** Methane seeps commonly harbor a wide range of taxonomically distinct ANME-
302 clades (e.g. 26, 37, 47, 48). The activity patterns and niche differentiation of these apparently
303 functionally redundant groups are, however, not understood. So far, temperature (31), CH₄
304 partial pressure (31), concentration of sulfate (32, 33) and sulfide (33), and nitrogen availability
305 (34, 35) have directly or indirectly been shown to drive the abundance and activity of different

306 ANME-lineages. Using BONCAT, we were able to demonstrate that representatives of all major
307 ANME-subpopulations (ANME-1 and ANME-2a, -2b, and -2c) co-occurring in a sediment
308 incubation were biosynthetically active under controlled AOM incubation conditions in the lab
309 (Tab. 1). This result raises questions about the ecology underlying this apparent functional
310 redundancy and factors influencing niche specialization. A promising approach for future studies
311 of the functional capacities and niche adaptations of different ANME-lineages will be to employ
312 isotopically labeled substrates in combination with BONCAT-based activity-screening in
313 targeted physiological experiments (9).

314 **Activity of ANME-SRB consortia in the absence of CH₄.** To date, members of ANME
315 archaea have only been shown to conserve energy through methane oxidation. Some studies,
316 however, have suggested that select ANME-populations might be capable of methanogenesis
317 (33, 49-53). Anabolic activity of individual ANME-SRB consortia in the absence of CH₄ has,
318 however, yet not been directly demonstrated. In our BONCAT-FISH studies, we found that after
319 30 days of incubation without the addition of CH₄, 7.9% of DAPI-stained microbial aggregates
320 from sediment #3730 were BONCAT-stained, and after 114 days, this proportion nearly doubled
321 to 14.6% (~50-95% of doubling time; 39, 40, 41). A similar trend was observed for sample
322 #7135 (14.5%, 30.4%, and 24.2% BONCAT-positive aggregates after 7, 41, and 171 days). This
323 observation was in stark contrast to our #7136-37 in incubations in the absence of methane, in
324 which only a very small percentage (2.3%) of microbial aggregates were fluorescently labeled.
325 While #3730 and #7135 consortia were clearly BONCAT-stained, their fluorescence intensity
326 was roughly 10-fold lower (n=20) than consortia incubated in the presence of CH₄. Consistent
327 with samples incubated in the presence of CH₄, the relative proportion of BONCAT-stained
328 aggregates that could be attributed to a specific ANME-population via (CARD)FISH was also
329 very low in the absence of CH₄ (0.3-9.8%, Fig. 2).

330 An explanation for activity of AOM-consortia in the absence of CH₄ headspace could be that
331 some consortia may have the potential to consume previously accumulated energy storage
332 compounds. This is supported by the observation that some representatives of ANME-2b but not
333 ANME-2c cells feature polyphosphate granules (McGlynn *et al.*, in prep.). Similarly, some
334 ANME-associated SRB might harbor carbon storage compounds (54). Our results suggest that
335 more AOM-consortia than previously thought are able to build up substantial amounts of energy
336 storage during times of substrate depletion. This is surprising, given the very low energy yield of
337 the AOM-reaction ($\Delta G^0 = -16 \text{ kJ mol}^{-1}$ at standard conditions) (55). Our finding, however, is
338 consistent with the observation that some AOM-consortia are able to invest substantial amounts
339 of metabolic energy in N₂-fixation (34, 56), one of the most energy-intensive reactions known
340 (16 ATP per N₂).

341 The observation of an increase in active consortia in sediment #3730 over long periods of
342 time (from 7.9% after 30 days to 14.7% after 114 days; Fig. 2) is, however, inconsistent with the
343 predicted progressive depletion of storage compounds. Another possible explanation for results
344 from #3730 could be attributed to an internal CH₄-cycle, in which methanogens produced CH₄,
345 which was then re-oxidized by AOM-consortia. Alternatively, members of ANME-SRB

346 consortia might themselves engage in the production of CH₄ rather than in sulfate-coupled AOM,
347 as previously suggested (49-53). Recent experiments on the methanogenic potential of ANME-1
348 and ANME-2 enrichment cultures, however, have not supported this idea (57). A minor amount
349 of CH₄ was detected in our N₂-containing #3730 and #7136-37 microcosms, however these
350 levels were similar to concentrations measured as a trace contaminant in the N₂-tank
351 (approximately 1-10 ppm CH₄). The reported CH₄ partial pressures capable of supporting AOM
352 by methane seep consortia is 1 bar (*i.e.* 1.4 mM in solution) (31, 43), 5 orders of magnitude
353 higher than concentrations in our incubations. Another intriguing possibility to explain the
354 activity of BONCAT-stained ANME-SRB consortia in the absence of CH₄ is that we yet might
355 not recognize the full extent of physiological capabilities of ANME-SRB consortia and that they
356 might be involved in energy conservation pathways unrelated to the oxidation or generation of
357 CH₄. A first step towards formulating hypotheses about potential energy-yielding substrates is to
358 identify specific archaeal-bacterial partnerships that might differ in their substrate range for
359 targeted genomics.

360 **Identification of microbial partners within activity-sorted consortia.** With few notable
361 exceptions (10, 11, 38, 58-60), single cell genome sequencing efforts so far have been “target-
362 blind”; they did not select for a specific taxon of interest or focus on metabolically active cells
363 that could be considered key species for ecosystem functioning. The power of these techniques
364 to investigate microbial partnerships involved in AOM was recently demonstrated by the
365 separation of FISH-identified ANME-consortia from methane seep sediments via immuno-
366 magnetic capture (magneto-FISH; 38, 61) and fluorescent-activated cell-sorting (FISH-FACS;
367 59, 62). Using sorting approaches, new associations between ANME and bacteria not known to
368 be capable of sulfate reduction, including members of the alpha-, beta-, gamma- and epsilon-
369 proteobacteria as well as *Planctomyces*, have been revealed (38). In addition, the potential of
370 targeted sorting approaches for uncovering rare populations has been demonstrated by the
371 successful enrichment of an ANME-2d population from ~2 to ~94% (59).

372 To demonstrate the potential of BONCAT to separate the functionally active fraction of a
373 microbial community from complex samples, we sorted individual, translationally active
374 consortia from sediments #3730 and #7142 by fluorescence-activated cell-sorting (FACS). We
375 refer to this activity-based cell-sorting approach as BONCAT-FACS (Fig. 1C). To test the
376 specificity of the chosen gates, 200 events per gate were sorted into individual tubes and
377 analyzed using fluorescence microscopy. For the BONCAT++ gate, which was used for all
378 downstream analyses, 204 DAPI-stained microbial aggregates were identified, all of which were
379 BONCAT-stained (Fig. 4). The slightly higher number of consortia (204 vs. the expected 200)
380 may be due to co-sorting of physically attached aggregates or the partial disaggregation of some
381 aggregates after sorting.

382 Consortia sorted into individual wells of micro-titer plates were lysed and their genomes
383 amplified via multiple displacement amplification (MDA) following established protocols (63).
384 For ethanol-fixed biomass from sediment #3730, 76 out of 168 sorted events resulted in a MDA
385 product. This efficiency (45%) is comparable with that of a recent study that reported a success

386 rate of 50% when DNA from cells stored in 70% EtOH was used as PCR template (64). By
387 avoiding any cell fixation prior to sorting of individual consortia (Fig. 4), the efficiency of MDA
388 reactions improved to 93% (78 out of 84 sorted events) for the same sample. Together, these
389 results suggest that BONCAT and click chemistry-mediated dye-labeling have no detrimental
390 effect on DNA-quality. Fixation of biomass was avoided for sediment #7142.

391 Diluted DNA from MDA reactions was used as the template in PCR amplifications targeting
392 the V4 region of archaeal and bacterial 16S rRNA genes (65, 66). Amplicons from PCR
393 reactions that yielded a single band during gel electrophoresis examination were barcoded,
394 sequenced, and phylogenetically analyzed (Fig. 5A and Fig. S6). The majority of reactions
395 contained both ANME- and SRB-related sequences in high numbers. In several reactions,
396 however, only sequences from either the ANME- or the SRB-partner were obtained (sequences
397 from the other cell type were <0.1%). Given the observed specificity for active microbial
398 aggregates of our sorting approach (Fig. 4B), preferential amplification of a single sequence type
399 for this subset may be indicative of bias during cell lysis and/or the MDA reaction, a problem
400 well discussed in the literature (64, 67, 68). Reactions that only recovered SRB sequences (n=5)
401 were not considered further in our analysis. For each of the remaining 45 consortia, a single
402 ANME operational taxonomic unit (OTU; defined here as a unique sequence) represented 93-
403 100% of all ANME-associated sequences. Similarly, in each individual consortium from
404 sediment #3730 a single OTU always contributed 94-100% of all SRB-related sequences.
405 Despite the relatively low number of consortia analyzed (n=34), representatives of the all
406 ANME-clades found in #3730 samples (according to 16S rRNA iTAG data) were retrieved from
407 a single incubation, corroborating the findings of phylogenetic diversity from our BONCAT-
408 FISH studies (findings are summarized in Tab. 1). Consistent with previous reports (26, 35, 38,
409 47, 69), ANME-1 and ANME-2 were predominantly associated with putative sulfate reducers
410 within the delta-proteobacterial lineages *Desulfobacterium*, *Desulfobulbus*, *Desulfococcus*, and
411 *Desulfosarcina* (Fig. 5A and FIG. S6). Analysis of single consortia further revealed that
412 individual ANME-subpopulations (single OTU) are often associated with different bacterial
413 partners, and *vice versa*. For example, the seven observed #3730 ANME-2b consortia (identical
414 in their V4 region) have partners within three different bacterial families. Similarly, three
415 consortia (A03Uf, C08Uf, and H01Uf) from sediment #7142 each harbored two SRB OTUs
416 (94.9-98.8% identical in sequence).

417 In addition to sequences from SRB, 5 consortia from sediment #3730 also yielded low
418 proportions of sequences from bacteria related to *Pseudomonas* or other gamma-proteobacteria
419 (Fig. 5A and FIG. S6). These sequences were taxonomically different than commonly observed
420 lab-contaminants and were distinct from sequences detected in over-amplified negative controls
421 or control mock communities. This result, together with (i) the finding of highly similar gamma-
422 proteobacterial sequences in a magneto-FISH study of AOM-consortia (38), (ii) our
423 demonstration that translationally active gamma-proteobacteria and archaea form consortia in
424 sediment #3730 (Tab. S2), and (iii) the observation that individual ANME-OTUs in different
425 consortia were associated with diverse bacterial groups, lend strong support to the idea that

426 AOM-partnerships are dynamic, both in terms of partner affiliation and possibly their
427 ecophysiology (38).

428 **Discovery of a new inter-domain partnership.** rRNA gene sequences obtained from an
429 ANME-1a consortium (#E06) from #3730 did not contain sequences related to known sulfate
430 reducers, but instead recovered sequences associated with *Verrucomicrobia*. Sequences retrieved
431 from a second consortium (#D05) also contained the same ANME-1a OTU, in addition to both
432 *Desulfobulbaceae* sequences and another *Verrucomicrobia*-affiliated OTU (sequence 80%
433 identical to the E06 OTU). Both *Verrucomicrobia*-affiliated sequences had $\leq 81\%$ identity to
434 rRNA genes from previously described species (Fig. 5A and FIG. S6).

435 To complement our sequence-based observations, we used FISH to screen 27 samples from 9
436 methane seep sediment cores obtained from a variety of geographic locations as well as two
437 carbonates retrieved from a methane vent site for the association of *Verrucomicrobia* with AOM-
438 consortia. We used two 16S rRNA-targeted probes specific for the phylum *Verrucomicrobia*
439 (EUB338-III and Ver47) (70-72), in combination with the general archaeal probe Arch915 to
440 screen archaeal aggregates from these samples. In four sediments (#3730 incubated for 30 and
441 114 days in the presence of HPG and CH₄; sediments #5119, #5202, and #7142) as well as both
442 carbonate samples (#2450 and #3439), verrucomicrobial cells were associated with 10-20% of
443 AOM-consortia (Tab. S3; Fig. S7). While the vast majority (~98%) of these aggregates
444 contained only low numbers of *Verrucomicrobia* (<20 per aggregate), a small number (n=14) of
445 aggregates exhibited very high ratios of verrucomicrobial to archaeal cells (Fig. 5; Fig. S7; Tab.
446 S3).

447 Despite the near-ubiquitous distribution of *Verrucomicrobia* in marine sediments (73),
448 including all 23 methane seeps recently surveyed via 16S i-tag sequencing (37), archaeal-
449 verrucomicrobial associations have not been described previously. Because of the loss of
450 structural information during DNA-extraction and the typically low abundance of consortia
451 consisting of ANME and non-traditional partner bacteria (38; Trembath-Reichert, in prep.; and
452 this study), metagenomic sequencing has yet failed to provide metabolic predictions on the
453 whole diversity of these microbial associations. This reinforces the imperative to combine
454 genomic sequencing with spatially resolved approaches, such as microscopy and cell-sorting
455 (e.g. 10, 67, 74), to gain access to the genetic potential of these important associations.

456 At this time, we can only speculate about the biological necessities driving the physical
457 association of *Verrucomicrobia* with ANME. The low relative abundance of *Verrucomicrobia*
458 associated with AOM-consortia, however, suggests that these cells might be heterotrophs,
459 consuming organic exudates or exo-polymers of the archaeal cells. A similar cross-feeding
460 relationship has previously been hypothesized for anammox bacteria co-occurring with ANME-
461 2d archaea (45). Genomic sequencing of individual ANME-*Verrucomicrobia* aggregates sorted
462 via BONCAT-FACS combined with additional microcosm experiments may assist with
463 expanding our understanding of the nature of these ANME-verrucomicrobial interactions.

464

465 **Conclusion and Outlook**

466 The possibility to detect anabolic activity of taxonomically identified cells using
467 fluorescence-staining offers a valuable compliment to existing fluorescence microscopy methods
468 for microbial ecology. BONCAT-FISH allows the activity-screening of thousands of cells within
469 a few hours, rather than a few dozen per day as achieved by isotope-labeling techniques. Both
470 bioorthogonal (this study) as well as non-destructive isotope-labeling (10, 58) approaches further
471 allow the sorting of individual cells and aggregates from complex samples, although sorting
472 throughput for BONCAT-FACS is much higher. Sorted cells can be subjected to whole genome
473 amplification and sequencing, thus allowing direct access to the genetic potential of cells
474 functionally important under defined conditions. In contrast to isotope labeling approaches,
475 which test whether cells are able to assimilate a specific substrate of interest (1, 5, 6, 75),
476 BONCAT is an un-targeted marker of translational activity. Hence, BONCAT cannot directly
477 provide information about specific substrate metabolism as is possible with SIP. However, the
478 possibility to combine BONCAT-incubations with the addition of any other compound allows
479 for *in situ* metabolic screening and comparative analysis of organisms stimulated by the
480 compound (9). Thus, we anticipate that BONCAT-FISH will be particularly attractive if non-
481 assimilatory pathways or substrates that are not (or only very expensively) available as stable
482 isotope-labeled derivatives are to be studied. Growth-promoting substrates could in the following
483 be used for the targeted cultivation of translationally responsive cells. In contrast to isotope
484 labeling approaches, which require specialized instrumentation, BONCAT-FISH and BONCAT-
485 FACS use standard-configuration microscopes and flow-cytometers that are more readily
486 available to molecular biological labs.

487 Here, we established that HPG at concentrations up to 50 μM can be applied to marine
488 methane seep sediments without detectable effects on the structure and function of the microbial
489 community. We demonstrate that the subsequent detection of HPG-containing *de novo*
490 synthesized proteins via click chemistry is a powerful approach to visualizing and identifying
491 translationally active microbes *in situ*, separating them from complex samples via activity-based
492 cell-sorting, and studying microbial interactions. We demonstrate that representatives of all
493 major subgroups of ANME are functionally active in Hydrate Ridge seep sediments. In addition,
494 we show that in two geographically distinct sediments some consortia are active in the absence
495 of CH_4 . It remains to be tested whether these findings are entirely the result of the use of cellular
496 storage materials or a physiological flexibility of these archaea that is yet unaccounted for.
497 Furthermore, we provide the first evidence for the existence of previously unrecognized
498 interactions of archaea and *Verrucomicrobia* in marine sediments. We anticipate that genomic
499 characterizations of these as well as other diverse ANME-SRB consortia will soon provide
500 hypotheses about potential growth-supporting substrates, and that BONCAT-FISH and
501 BONCAT-FACS will play important roles in experimentally testing the ecophysiological
502 properties of these globally relevant microbial partnerships.

503

504 **Materials and Methods**

505 **Incubation of methane seep sediment.** Samples were obtained from three sediment cores
506 taken off the coasts of California (Santa Monica Basin) and Oregon (Hydrate Ridge) and
507 incubated in the presence of absence of *L*-homopropargylglycine (HPG) and CH₄ for up to 6
508 months. Samples for geochemical characterization, whole-community composition, and
509 microscopic analyses were taken in regular intervals. Details on these experimental procedures
510 are described in the *SI Appendix*.

511 **Bioorthogonal non-canonical amino acid tagging (BONCAT).** BONCAT was performed
512 following our recently established protocol without modifications (44). Succinctly, fixed biomass
513 (whole sediment or extracted consortia) was immobilized on Teflon-coated glass-slides and dried
514 at 46°C. An increasing ethanol series (50, 80, and 96% ethanol in ddH₂O) was performed and the
515 slides air-dried. Solutions were prepared as recently described (44) and the “click cocktail” was
516 always freshly mixed. This solution contained 5 mM sodium ascorbate (Sigma-Aldrich), 5 mM
517 amino-guanidine hydrochloride (Sigma-Aldrich), 500 μM Tris[(1-hydroxypropyl)-1H-1,2,3-
518 triazol-4-yl)methyl]amine (THPTA; Click Chemistry Tools), 100 μM CuSO₄ (Sigma-Aldrich)
519 and 2 μM of azide-modified dye carboxyrhodamine 110 (CR-110; Click Chemistry Tools) or
520 azide-modified 5(6)-carboxytetramethylrhodamine (TAMRA; Click Chemistry Tools) [used only
521 in combination with CARD-FISH] in 0.2 μm-filtered 1x PBS, pH 7.4. 20 μL of this solution
522 were applied atop of biomass and the glass slides incubated for 60 min at RT in a humid
523 chamber. Afterwards, slides were washed repeatedly in 1x PBS and an increasing ethanol series
524 (50, 80, and 96%), before being air-dried. For details on this protocol see Hatzenpichler and
525 Orphan (2015) and Hatzenpichler *et al.* (2014). Non-fixed samples were processed following the
526 same protocol with the difference that all ethanol-washing steps were omitted.

527 **Fluorescence *in situ* hybridization (FISH) and Catalyzed Reporter Deposition (CARD)**
528 **FISH.** Following BONCAT, ethanol-washed samples were hybridized with oligonucleotide-
529 probes. For FISH-experiments, double- (76) or mono-labeled probes with either Cy3 or Cy5
530 fluorescence dyes were used. FISH hybridizations were performed overnight (14-18 hours)
531 according to standard protocols (9, 77). The quality of all probe solutions (except ANME-2-932)
532 was checked using other seep samples before they were applied to #3730 and #7135-37
533 sediments. All tested probe solutions yielded a large number of positive hybridizations to AOM-
534 consortia in these control samples. Each probe or probe-set was hybridized in a technical
535 duplicate or triplicate. No differences in fluorescence intensity or relative proportion of
536 (CARD)FISH-positive consortia could be observed between replicate hybridizations.

537 **CARD-FISH** was performed as recently described (78). Three different cell wall digestion
538 protocols were tested, but only one, a modified version of a recently published protocol (35), was
539 found to be successful. Permeabilization was performed at RT as follows: incubation in 0.01 M
540 HCl for 15 min; 2 washing steps in water, 1 min each; incubation in 0.5% sodium-dodecyl
541 sulfate for 5 min; 3 washing steps in water, 1 min each; incubation in 50% EtOH for 1 min. After
542 air-drying, samples were hybridized for 14-18 with horseradish peroxidase-conjugated

543 oligonucleotides (purchased from Biomers), before signal amplification using self-synthesized
544 fluorescein-labeled tyramide was carried out.

545 **Microscopy and image analysis.** Samples were mounted with 1 mg mL⁻¹ 4,6-diamidino-2-
546 phenylindole (DAPI; Sigma-Aldrich) in Citifluor AF-1 anti-fading solution (Electron
547 Microscopy Sciences) and analyzed using either an Olympus BX51 epifluorescence microscope
548 or a Zeiss LSM-510-Meta confocal laser-scanning microscope. Images were analyzed using the
549 imageJ software (NIH). In total, 12,652, 2,232, and 1,554 consortia were analyzed for sediment
550 #3730, #7135, and #7136-37, respectively. The lower number of consortia analyzed for the latter
551 samples is explained by the much lower concentration of AOM-consortia in that sediment core.
552 Each DAPI-stained microbial aggregate was manually inspected for BONCAT- and FISH-
553 signals, and representative images were taken for each probe-set. Consortia were always
554 identified via DAPI, before switching to the other fluorescent channels to not preferentially
555 select for BONCAT-positive or FISH-positive consortia. A detailed list of BONCAT-FISH
556 counts can be found in the Tab. S2 and Tab. S3. In every BONCAT-positive aggregate either (i)
557 (nearly) all cells within an aggregate were stained, or, in rare cases, (ii) (nearly) all cells of one
558 (but not the other) cell-type (archaea or bacteria) were stained. Given the complex three-
559 dimensional structure of the aggregates, which sometimes grow many thousands of cells large
560 (see Fig. 2A), we cannot exclude that in rare cases individual cells (<5%) of a specific cell-type
561 were not stained (hence, the term “nearly all”).

562 After shipping and storage at 4°C for three days, activity-sorted consortia were re-suspended
563 in 1 mL 1x PBS, before being harvested by centrifugation (5 min at 16,100 g, RT), re-suspended
564 in 1:1 1x PBS:EtOH, and immobilized on a glass slide. The slide was washed for 1 min in 50%
565 EtOH (in ddH₂O), air-dried, DAPI-embedded, and microscopically analyzed. Consortia were
566 counted following the same procedure as outlined above and representative images were taken.

567 **Activity-based cell-sorting.** Initial tests were performed using pure cultures and mixtures of
568 *Escherichia coli* K-12, *Methyloprofundus sedimenti* WF-1 (79), and *Desulfovibrio alaskensis*
569 G20 that had been incubated in the absence or presence (250 μM) of HPG for ~1 generation and
570 stained using an azide-modified version of dye CR110 as recently described (9, 44). After
571 successful tests, BONCAT-treated sediment-extracted consortia from samples #3730 and #7142
572 were analyzed. A BD Influx cell sorter was sterilized, and sheath fluid was prepared using 1x
573 PBS as recently described (63). After passing through a 70 μm nylon mesh filter, samples were
574 sorted using a 200 μm nozzle at 0.21 bar. The sort mode was “1.0 drop single”. 2x 84 single
575 events were deposited into wells E4-L15 of two 384-well plates, with Rows D and L serving as
576 negative control wells. BONCAT-dye CR110 was excited using a 488 nm laser and fluorescence
577 was captured with a 531 nm / 30 nm filter. Gates were defined using a forward scatter (FSC) vs.
578 531 nm emission plot, and events with a BONCAT signal brighter than >90% of aggregates in
579 the negative control were captured (see Fig. 4). For quantification of sorted consortia, 200 events
580 identified within each gate were sorted into 1.5 mL tubes that contained 10 μL 1x PBS. Tubes
581 were stored at 4°C until further processing.

582 **Sequence access.** Sequences have been deposited in the National Center for Biotechnology
583 Information database under accession numbers KT945170-KT945234 and KU564217-
584 KU564240 (16S rRNA iTAG sequences from activity-sorted consortia in #3730 and #7142,
585 respectively) and SRP066109 (whole community 16S rRNA iTAG sequences).

586

587

588

589 **Acknowledgements**

590 We thank Alexis Pasulka and Kat Dawson for providing sediment samples, Silvan Scheller
591 and Kat Dawson for measurements of AOM-rates and methane concentrations, Hang Yu for
592 performing cline assays, Connor Skennerton for help during sampling of sediment incubations,
593 David Case for discussions on tag-sequences analyses, and Shawn McGlynn for discussions on
594 storage compounds. David Case, Kat Dawson, and Elizabeth Wilbanks are acknowledged for
595 critical comments on the ms. We thank The Biological Imaging Facility of Caltech for access to
596 their confocal microscope. Roland Hatzepichler was supported via Erwin Schrödinger
597 Postdoctoral Fellowship J 3162-B20 of the Austrian Science Fund (FWF) and a Postdoctoral
598 Fellowship by the Center for Dark Energy Biosphere Investigations (C-DEBI). Funding for this
599 project was provided by the Gordon and Betty Moore Foundation through Grant GBMF3780 to
600 VJO, grant DE-PS02-09ER09-25 from the Department of Energy to VJO, and a JGI Director
601 Discretionary Project Award to RH and VJO. The work conducted by the U.S. Department of
602 Energy Joint Genome Institute, a DOE Office of Science User Facility, is supported under
603 Contract No. DE-AC02-05CH11231. This is C-DEBI contribution XXX (number to be added in
604 proof).
605

606 **Figure legends**

607

608 **Fig. 1.** Concept for the visualization, identification, and sorting of translationally active cells.
609 (A) The bioorthogonal amino acid *L*-homopropargylglycine (HPG) is added to an environmental
610 sample, which is then incubated under *in situ* conditions. After HPG has entered the cell, the
611 exact process of which is currently unknown, it competes with methionine (Met) for
612 incorporation into newly made peptides. HPG-containing proteins are then fluorescently labeled
613 via a Cu(I)-catalyzed azide-alkyne click reaction, thus marking cells that have undergone protein
614 synthesis during time of incubation. (B) Next, rRNA-targeted fluorescence *in situ* hybridization
615 (FISH) is performed to taxonomically identify anabolically active cells. In this example, the
616 yellow cell is detected via both BONCAT and FISH, while the other two were either not
617 translationally active (red cell) or are taxonomically unidentified but active (green cell). (C)
618 Individual labeled cells or consortia can be separated using fluorescence-activated cell-sorting
619 (FACS). Cells are lysed and their genomes amplified using multiple displacement amplification
620 (MDA). The resulting amplified genomes are taxonomically screened via amplification and
621 sequencing of the V4 region of the 16S rRNA gene. This information may then guide the
622 selection of cells or consortia for genomic sequencing.

623

624 **Fig. 2.** Temporal dynamics of translational activities of microbial consortia as revealed by
625 BONCAT-FISH. Three geographically distinct sediment samples, #3730, #7135, and #7136-37
626 were incubated in the presence of CH₄ or N₂ for 114, 171, and 31 days, respectively. 2.3-30.4%
627 of aggregates were translationally active in absence of CH₄, suggesting either the use of storage
628 compounds, the presence of an endogenous methane source, or a potential physiological
629 flexibility of these microbial partnerships. Green bars show the relative abundance of aggregates
630 detectable via BONCAT. Red bars indicate the detection rate of DAPI-stained aggregates by
631 FISH and CARD-FISH. Yellow bars give the relative abundance of aggregates that were both
632 BONCAT-positive as well as FISH- or CARD-FISH stained. n, number of microbial aggregates
633 analyzed per experiment. For a list of probes and detailed results, see Tab. S2.

634

635 **Fig. 3.** Single cell-resolved visualization of the translational activity of morphologically and
636 taxonomically distinct methane-oxidizing consortia in sediment #3730. Protein synthesis-active
637 cells were identified via BONCAT (green). 16S rRNA-targeted oligonucleotide FISH-probes,
638 specific for the domain *Archaea* (A,B), most delta-proteobacteria (C,F), and ANME-subgroup 2b
639 (D,E), were used to taxonomically identify the two microbial partners (red). DAPI-staining of
640 DNA is shown in blue. An overlay of the three fluorescence channels and a 10 μm scale bar are
641 shown in the lower right image of each panel. BONCAT-negative cells were either
642 translationally inactive or have not taken up or incorporated HPG into new proteins.

643

644 **Fig. 4.** Flow cytometric analysis of unfixed microbial cells and consortia extracted from
645 sediment #3730 after incubation with (A) or without (B) of HPG. (C) Microbial consortia

646 detected by fluorescence microscopy after sorting of 200 events per gate. (A). Only ‘BONCAT’
647 and ‘BONCAT++’ gates were used for activity-based sorting. Microscopic images of
648 representative tube-sorted consortia are on the right. Note that the relative fluorescence intensity
649 differs between gates (for gate ‘P1’ events, exposure time had to be increased 10-fold as
650 compared to gate ‘BONCAT’ to yield visually detectable BONCAT-fluorescence). FSC, forward
651 scatter; RFI 488nm, relative fluorescence intensity at an excitation of 488 nm; ‘BONCAT++’,
652 ‘BONCAT’, ‘P1’, ‘P2’, and ‘P3’, gates using for counting and sorting; Gate ‘P3’ did only
653 contain individual cells as well as sediment and Percoll particles. Percent-values indicate the
654 relative abundance of events within each gate.

655
656 **Fig. 5.** Identification of microbial partners within AOM-consortia after activity-based
657 sorting. Taxonomic affiliation of the archaeal (left) and bacterial (right) partners within 45
658 individually sorted, translationally active consortia from sediments #3730 (black) after 114 days
659 and #7142 (red) after 25 days of incubation with HPG. The potential to discover yet
660 unrecognized microbial interactions with this approach is evidenced by our finding of two
661 consortia containing *Verrucomicrobia*-derived sequences. Using FISH, we independently
662 confirmed the presence and activity of microbial consortia composed of *Archaea* and
663 *Verrucomicrobia* in several sediment and carbonate samples. Trees represent maximum
664 likelihood reconstructions onto which bootstrap values are projected. Green and white colored
665 boxes show support $\geq 90\%$ and $\geq 70\%$, respectively. Values $< 70\%$ are not shown. Left and right
666 boxes indicate max. parsimony (100x) and neighbor joining (1,000x) values, respectively. Tag
667 sequences were added after tree construction without changing overall tree topology. Solid and
668 dashed lines indicate individual archaeal-bacterial partnerships. Scale bars equal 10% estimated
669 sequence divergence. Detailed trees and additional FISH-images are available in the SOI (Fig.
670 S6 and S7).

671

672 **References**

- 673 1. Neufeld JD, Wagner M, Murrell JC (2007) Who eats what, where and when? Isotope-
674 labelling experiments are coming of age. *ISME J* 1(2):103-110.
- 675 2. Moran MA, *et al.* (2013) Sizing up metatranscriptomics. *ISME J* 7(2):237-243.
- 676 3. VerBerkmoes NC, Deneff VJ, Hettich RL, Banfield JF (2009) Functional analysis of natural
677 microbial consortia using community proteomics. *Nature Reviews Microbiology* 7(3):196-
678 205.
- 679 4. Orphan VJ (2009) Methods for unveiling cryptic microbial partnerships in nature. *Current*
680 *Opinion in Microbiology* 12(3):231-237.
- 681 5. Wagner M (2009) Single-cell ecophysiology of microbes as revealed by Raman
682 microspectroscopy or secondary ion mass spectrometry imaging. *Annu Rev Microbiol*
683 63:411-429.
- 684 6. Lee N, *et al.* (1999) Combination of fluorescent in situ hybridization and
685 microautoradiography-a new tool for structure-function analyses in microbial ecology.
686 *Appl Environ Microbiol* 65(3):1289-1297.
- 687 7. Orphan VJ, House CH, Hinrichs KU, McKeegan KD, DeLong EF (2001) Methane-
688 consuming archaea revealed by directly coupled isotopic and phylogenetic analysis.
689 *Science* 293(5529):484-487.
- 690 8. Huang WE, *et al.* (2007) Raman-FISH: combining stable-isotope Raman spectroscopy and
691 fluorescence in situ hybridization for the single cell analysis of identity and function.
692 *Environ Microbiol* 9(8):1878-1889.
- 693 9. Hatzenpichler R, *et al.* (2014) *In situ* visualization of newly synthesized proteins in
694 environmental microbes using amino acid tagging and click chemistry. *Environ Microbiol*
695 16(8):2568-2590.
- 696 10. Berry D, *et al.* (2014) Tracking heavy water (D2O) incorporation for identifying and
697 sorting active microbial cells. *Proc Natl Acad Sci U S A* 112(2):E194-203.
- 698 11. Kalyuzhnaya MG, Lidstrom ME, Chistoserdova L (2008) Real-time detection of actively
699 metabolizing microbes by redox sensing as applied to methylotroph populations in Lake
700 Washington. *ISME J* 2(7):696-706.
- 701 12. Konopka MC, *et al.* (2011) Respiration response imaging for real-time detection of
702 microbial function at the single-cell level. *Appl Environ Microbiol* 77(1):67-72.
- 703 13. Smriga S, Samo TJ, Malfatti F, Villareal J, Azam F (2014) Individual cell DNA synthesis
704 within natural marine bacterial assemblages as detected by 'click' chemistry. *Aquat Microb*
705 *Ecol* 72:269-280.
- 706 14. Samo TJ, Smriga S, Malfatti F, Sherwood BP, Azam F (2014) Broad distribution and high
707 proportion of protein synthesis active marine bacteria revealed by click chemistry at the
708 single cell level. *Front Mar Sci* doi: 10.3389/fmars.2014.00048.
- 709 15. Dieterich DC, *et al.* (2007) Labeling, detection and identification of newly synthesized
710 proteomes with bioorthogonal non-canonical amino-acid tagging. *Nat Protoc* 2(3):532-540.
- 711 16. Dieterich DC, Link AJ, Graumann J, Tirrell DA, Schuman EM (2006) Selective
712 identification of newly synthesized proteins in mammalian cells using bioorthogonal
713 noncanonical amino acid tagging (BONCAT). *Proc Natl Acad Sci U S A* 103(25):9482-
714 9487.
- 715 17. Kiick KL, Saxon E, Tirrell DA, Bertozzi CR (2002) Incorporation of azides into
716 recombinant proteins for chemoselective modification by the Staudinger ligation. *Proc Natl*
717 *Acad Sci U S A* 99(1):19-24.

- 718 18. Ngo JT, Tirrell DA (2011) Noncanonical amino acids in the interrogation of cellular
719 protein synthesis. *Acc Chem Res* 44(9):677-685.
- 720 19. Bagert JD, *et al.* (2014) Quantitative, Time-Resolved Proteomic Analysis by Combining
721 Bioorthogonal Noncanonical Amino Acid Tagging and Pulsed Stable Isotope Labeling by
722 Amino Acids in Cell Culture. *Mol Cell Proteomics* 13:1352-1358.
- 723 20. Sinai L, Rosenberg A, Smith Y, Segev E, Ben-Yehuda S (2015) The molecular timeline of
724 a reviving bacterial spore. *Mol Cell* 57(4):695-707.
- 725 21. Beatty KE, Tirrell DA (2008) Two-color labeling of temporally defined protein populations
726 in mammalian cells. *Bioorg Med Chem Lett* 18(22):5995-5999.
- 727 22. Dieterich DC, *et al.* (2010) In situ visualization and dynamics of newly synthesized
728 proteins in rat hippocampal neurons. *Nat Neurosci* 13(7):897-905.
- 729 23. Beatty KE, *et al.* (2006) Fluorescence visualization of newly synthesized proteins in
730 mammalian cells. *Angew Chem Int Ed Engl* 45(44):7364-7367.
- 731 24. Beatty KE, Xie F, Wang Q, Tirrell DA (2005) Selective dye-labeling of newly synthesized
732 proteins in bacterial cells. *J Am Chem Soc* 127(41):14150-14151.
- 733 25. Reeburgh WS (2007) Oceanic methane biogeochemistry. *Chem Rev* 107(2):486-513.
- 734 26. Boetius A, *et al.* (2000) A marine microbial consortium apparently mediating anaerobic
735 oxidation of methane. *Nature* 407(6804):623-626.
- 736 27. McGlynn SE, Chadwick GL, Kempes CP, Orphan VJ (2015) Single cell activity reveals
737 direct electron transfer in methanotrophic consortia. *Nature* doi:10.1038/nature15512.
- 738 28. Wegener G, Krukenberg V, Riedel D, Tegetmeyer HE, Boetius A (2015) Intercellular
739 wiring enables electron transfer between methanotrophic archaea and bacteria. *Nature*
740 526:587-590.
- 741 29. Milucka J, *et al.* (2012) Zero-valent sulphur is a key intermediate in marine methane
742 oxidation. *Nature* 491(7425):541-546.
- 743 30. Moran JJ, *et al.* (2008) Methyl sulfides as intermediates in the anaerobic oxidation of
744 methane. *Environmental Microbiology* 10(1):162-173.
- 745 31. Nauhaus K, Treude T, Boetius A, Kruger M (2005) Environmental regulation of the
746 anaerobic oxidation of methane: a comparison of ANME-I and ANME-II communities.
747 *Environ Microbiol* 7(1):98-106.
- 748 32. Yanagawa K, *et al.* (2011) Niche Separation of Methanotrophic Archaea (ANME-1 and -2)
749 in Methane-Seep Sediments of the Eastern Japan Sea Offshore Joetsu. *Geomicrobiol J*
750 28:118-129.
- 751 33. Timmers PH, Widjaja-Greefkes HC, Ramiro-Garcia J, Plugge CM, Stams AJ (2015)
752 Growth and activity of ANME clades with different sulfate and sulfide concentrations in
753 the presence of methane. *Frontiers in microbiology* 6:988.
- 754 34. Dekas AE, Poretsky RS, Orphan VJ (2009) Deep-sea archaea fix and share nitrogen in
755 methane-consuming microbial consortia. *Science* 326(5951):422-426.
- 756 35. Green-Saxena A, Dekas AE, Dalleska NF, Orphan VJ (2014) Nitrate-based niche
757 differentiation by distinct sulfate-reducing bacteria involved in the anaerobic oxidation of
758 methane. *ISME J* 8(1):150-163.
- 759 36. Knittel K, Losekann T, Boetius A, Kort R, Amann R (2005) Diversity and distribution of
760 methanotrophic archaea at cold seeps. *Appl Environ Microbiol* 71(1):467-479.
- 761 37. Ruff SE, *et al.* (2015) Global dispersion and local diversification of the methane seep
762 microbiome. *Proc Natl Acad Sci U S A* 112(13):4015-4020.

- 763 38. Pernthaler A, *et al.* (2008) Diverse syntrophic partnerships from deep-sea methane vents
764 revealed by direct cell capture and metagenomics. *Proc Natl Acad Sci U S A*.
- 765 39. Girguis PR, Orphan VJ, Hallam SJ, DeLong EF (2003) Growth and methane oxidation
766 rates of anaerobic methanotrophic archaea in a continuous-flow bioreactor. *Appl Environ*
767 *Microbiol* 69(9):5472-5482.
- 768 40. Nauhaus K, Albrecht M, Elvert M, Boetius A, Widdel F (2007) *In vitro* cell growth of
769 marine archaeal-bacterial consortia during anaerobic oxidation of methane with sulfate.
770 *Environ Microbiol* 9(1):187-196.
- 771 41. Orphan VJ, Turk KA, Green AM, House CH (2009) Patterns of ¹⁵N assimilation and
772 growth of methanotrophic ANME-2 archaea and sulfate-reducing bacteria within structured
773 syntrophic consortia revealed by FISH-SIMS. *Environ Microbiol* 11(7):1777-1791.
- 774 42. Larowe DE, Dale AW, Regnier P (2008) A thermodynamic analysis of the anaerobic
775 oxidation of methane in marine sediments. *Geobiology* 6(5):436-449.
- 776 43. Nauhaus K, Boetius A, Kruger M, Widdel F (2002) *In vitro* demonstration of anaerobic
777 oxidation of methane coupled to sulphate reduction in sediment from a marine gas hydrate
778 area. *Environ Microbiol* 4(5):296-305.
- 779 44. Hatzenpichler R, Orphan VJ (2015) Detection of protein-synthesizing microorganisms in
780 the environment via bioorthogonal non-canonical amino acid tagging (BONCAT).
781 *Hydrocarbon and Lipid Microbiology Protocols*, ed McGenity TJ (Springer, Berlin
782 Heidelberg), Vol Vol. 7: Single-cell and single-molecule methods.
- 783 45. Haroon MF, *et al.* (2013) Anaerobic oxidation of methane coupled to nitrate reduction in a
784 novel archaeal lineage. *Nature* 500(7464):567-570.
- 785 46. Behrens S, *et al.* (2003) *In situ* accessibility of small-subunit rRNA of members of the
786 domains *Bacteria*, *Archaea*, and *Eucarya* to Cy3-labeled oligonucleotide probes. *Appl*
787 *Environ Microbiol* 69(3):1748-1758.
- 788 47. Orphan VJ, *et al.* (2001) Comparative analysis of methane-oxidizing archaea and sulfate-
789 reducing bacteria in anoxic marine sediments. *Appl Environ Microbiol* 67(4):1922-1934.
- 790 48. Orphan VJ, House CH, Hinrichs KU, McKeegan KD, DeLong EF (2002) Multiple archaeal
791 groups mediate methane oxidation in anoxic cold seep sediments. *Proc Natl Acad Sci U S*
792 *A* 99(11):7663-7668.
- 793 49. Lloyd KG, Alperin MJ, Teske A (2011) Environmental evidence for net methane
794 production and oxidation in putative ANaerobic MEthanotrophic (ANME) archaea.
795 *Environ Microbiol* 13(9):2548-2564.
- 796 50. Orcutt B, Boetius A, Elvert M, Samarkin V, Joye SB (2005) Molecular biogeochemistry of
797 sulfate reduction, methanogenesis and the anaerobic oxidation of methane at Gulf of
798 Mexico cold seeps. *Geochimica Et Cosmochimica Acta* 69:4267-4281.
- 799 51. Treude T, *et al.* (2007) Consumption of methane and CO₂ by methanotrophic microbial
800 mats from gas seeps of the anoxic Black Sea. *Appl Environ Microbiol* 73(7):2271-2283.
- 801 52. Bertram S, *et al.* (2013) Methanogenic capabilities of ANME-archaea deduced from (13)
802 C-labelling approaches. *Environ Microbiol* 15(8):2384-2393.
- 803 53. House CH, *et al.* (2009) Extensive carbon isotopic heterogeneity among methane seep
804 microbiota. *Environ Microbiol* 11(9):2207-2215.
- 805 54. Heller C, Hoppert M, Reitner A (2008) Immunological localization of Coenzyme M
806 reductase in anaerobic methane-oxidizing Archaea of ANME 1 and ANME 2.
807 *Geomicrobiol J* 25:149-156.

- 808 55. Knittel K, Boetius A (2009) Anaerobic oxidation of methane: progress with an unknown
809 process. *Annu Rev Microbiol* 63:311-334.
- 810 56. Dekas AE, Connon SA, Chadwick GL, Trembath-Reichert E, Orphan VJ (2015) Activity
811 and interactions of methane seep microorganisms assessed by parallel transcription and
812 FISH-NanoSIMS analyses. *ISME J*.
- 813 57. Wegener G, Krukenberg V, Ruff SE, Kellermann MY, Knittel K (2016) Metabolic
814 Capabilities of Microorganisms Involved in and Associated with the Anaerobic Oxidation
815 of Methane. *Frontiers in microbiology* 7(doi: 10.3389/fmicb.2016.00046).
- 816 58. Huang WE, Ward AD, Whiteley AS (2009) Raman tweezers sorting of single microbial
817 cells. *Environ Microbiol Rep* 1(1):44-49.
- 818 59. Yilmaz S, Haroon MF, Rabkin BA, Tyson GW, Hugenholtz P (2010) Fixation-free
819 fluorescence *in situ* hybridization for targeted enrichment of microbial populations. *ISME J*
820 4(10):1352-1356.
- 821 60. Kashtan N, *et al.* (2014) Single-cell genomics reveals hundreds of coexisting
822 subpopulations in wild *Prochlorococcus*. *Science* 344(6182):416-420.
- 823 61. Trembath-Reichert E, Green-Saxena A, Orphan VJ (2013) Whole cell immunomagnetic
824 enrichment of environmental microbial consortia using rRNA-targeted Magneto-FISH.
825 *Methods Enzymol* 531:21-44.
- 826 62. Losekann T, *et al.* (2007) Diversity and abundance of aerobic and anaerobic methane
827 oxidizers at the Haakon Mosby Mud Volcano, Barents Sea. *Appl Environ Microbiol*
828 73(10):3348-3362.
- 829 63. Rinke C, *et al.* (2014) Obtaining genomes from uncultivated environmental
830 microorganisms using FACS-based single-cell genomics. *Nat Protoc* 9(5):1038-1048.
- 831 64. Clingenpeel S, Schwientek P, Hugenholtz P, Woyke T (2014) Effects of sample treatments
832 on genome recovery via single-cell genomics. *ISME J* 8(12):2546-2549.
- 833 65. Caporaso JG, *et al.* (2012) Ultra-high-throughput microbial community analysis on the
834 Illumina HiSeq and MiSeq platforms. *ISME J* 6(8):1621-1624.
- 835 66. Caporaso JG, *et al.* (2011) Global patterns of 16S rRNA diversity at a depth of millions of
836 sequences per sample. *Proc Natl Acad Sci U S A* 108 Suppl 1:4516-4522.
- 837 67. Rinke C, *et al.* (2013) Insights into the phylogeny and coding potential of microbial dark
838 matter. *Nature* 499(7459):431-437.
- 839 68. Clingenpeel S, Clum A, Schwientek P, Rinke C, Woyke T (2014) Reconstructing each
840 cell's genome within complex microbial communities-dream or reality? *Frontiers in*
841 *microbiology* 5:771.
- 842 69. Kleindienst S, Ramette A, Amann R, Knittel K (2012) Distribution and *in situ* abundance
843 of sulfate-reducing bacteria in diverse marine hydrocarbon seep sediments. *Environ*
844 *Microbiol* 14(10):2689-2710.
- 845 70. Daims H, Bruhl A, Amann R, Schleifer KH, Wagner M (1999) The domain-specific probe
846 EUB338 is insufficient for the detection of all *Bacteria*: development and evaluation of a
847 more comprehensive probe set. *Syst Appl Microbiol* 22(3):434-444.
- 848 71. Arnds J, Knittel K, Buck U, Winkel M, Amann R (2010) Development of a 16S rRNA-
849 targeted probe set for Verrucomicrobia and its application for fluorescence *in situ*
850 hybridization in a humic lake. *Syst Appl Microbiol* 33(3):139-148.
- 851 72. Bergen B, Herlemann DP, Labrenz M, Jurgens K (2014) Distribution of the
852 verrucomicrobial clade Spartobacteria along a salinity gradient in the Baltic Sea. *Environ*
853 *Microbiol Rep* 6(6):625-630.

- 854 73. Freitas S, *et al.* (2012) Global distribution and diversity of marine *Verrucomicrobia*. *ISME*
855 *J* 6(8):1499-1505.
- 856 74. Blainey PC (2013) The future is now: single-cell genomics of bacteria and archaea. *FEMS*
857 *Microbiol Rev* 37(3):407-427.
- 858 75. Orphan VJ, House CH (2009) Geobiological investigations using secondary ion mass
859 spectrometry: microanalysis of extant and paleo-microbial processes. *Geobiology* 7(3):360-
860 372.
- 861 76. Stoecker K, Dorninger C, Daims H, Wagner M (2010) Double labeling of oligonucleotide
862 probes for fluorescence in situ hybridization (DOPE-FISH) improves signal intensity and
863 increases rRNA accessibility. *Appl Environ Microbiol* 76(3):922-926.
- 864 77. Daims H, Stoecker K, Wagner M (2005) Fluorescence *in situ* hybridization for the
865 detection of prokaryotes. *Molecular Microbial Ecology*, eds Osborn AM & Smith CJ (Bios
866 Advanced Methods, Abingdon), pp 213-239.
- 867 78. Hatzenpichler R, *et al.* (2008) A moderately thermophilic ammonia-oxidizing
868 crenarchaeote from a hot spring. *Proc Natl Acad Sci U S A* 105(6):2134-2139.
- 869 79. Tavormina PL, *et al.* (2015) *Methyloprofundus sedimenti* gen. nov., sp. nov., an obligate
870 methanotroph from ocean sediment belonging to the 'deep sea-1' clade of marine
871 methanotrophs. *Int J Syst Evol Microbiol* 65(Pt 1):251-259.

872

Tab. 1. Comparison of 16S rRNA gene-based affiliations of ANME-related archaea in sediment #3730 after 114 days of incubation in the presence of CH₄ reveals that members of all ANME-subclade are active under controlled conditions.

Number of aggregates	FISH	CARDFISH	FACS
DAPI	2,946	1,130	
BONCAT+	1,922	678	34
CARD(FISH)+	167	48	
BONCAT+ and (CARD)FISH+	163	42	
% ANME 1	1	79	29
% ANME 2a	34	0	3
% ANME 2b	27	14	21
% ANME 2c	38	7	47

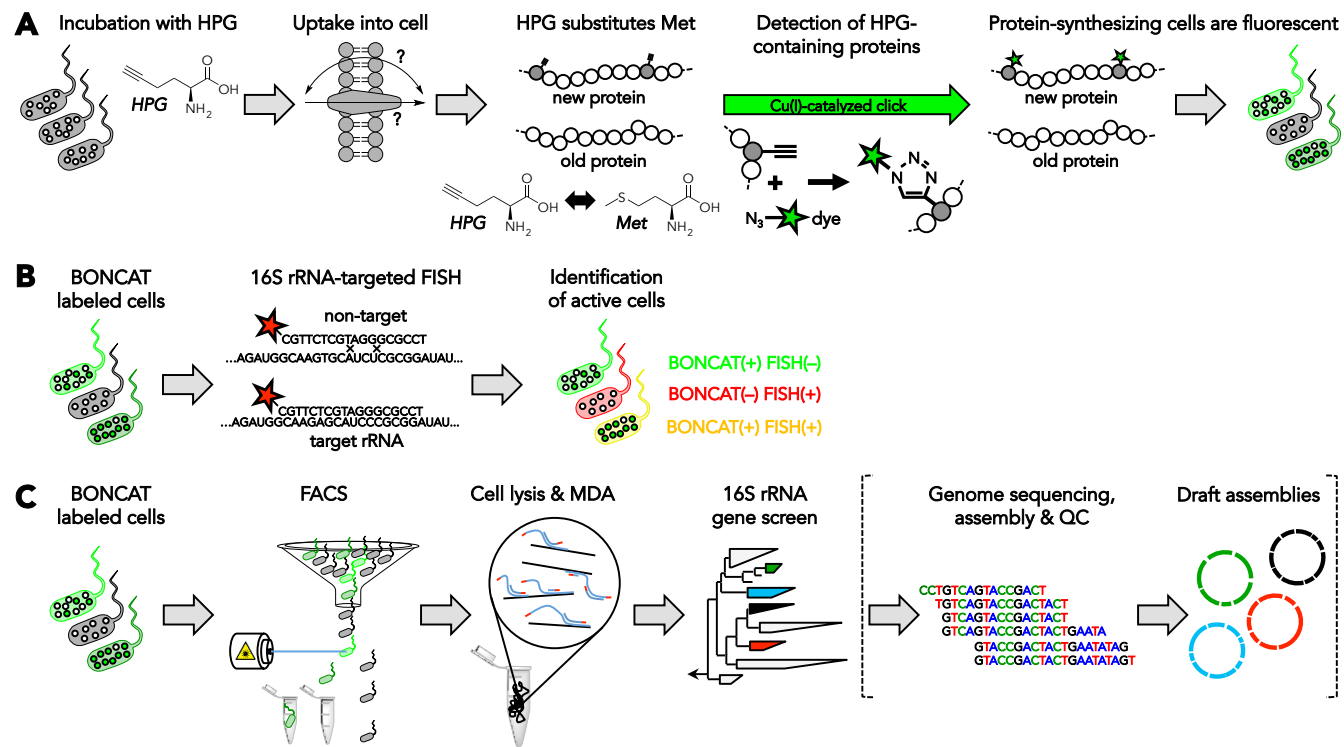


Figure 1

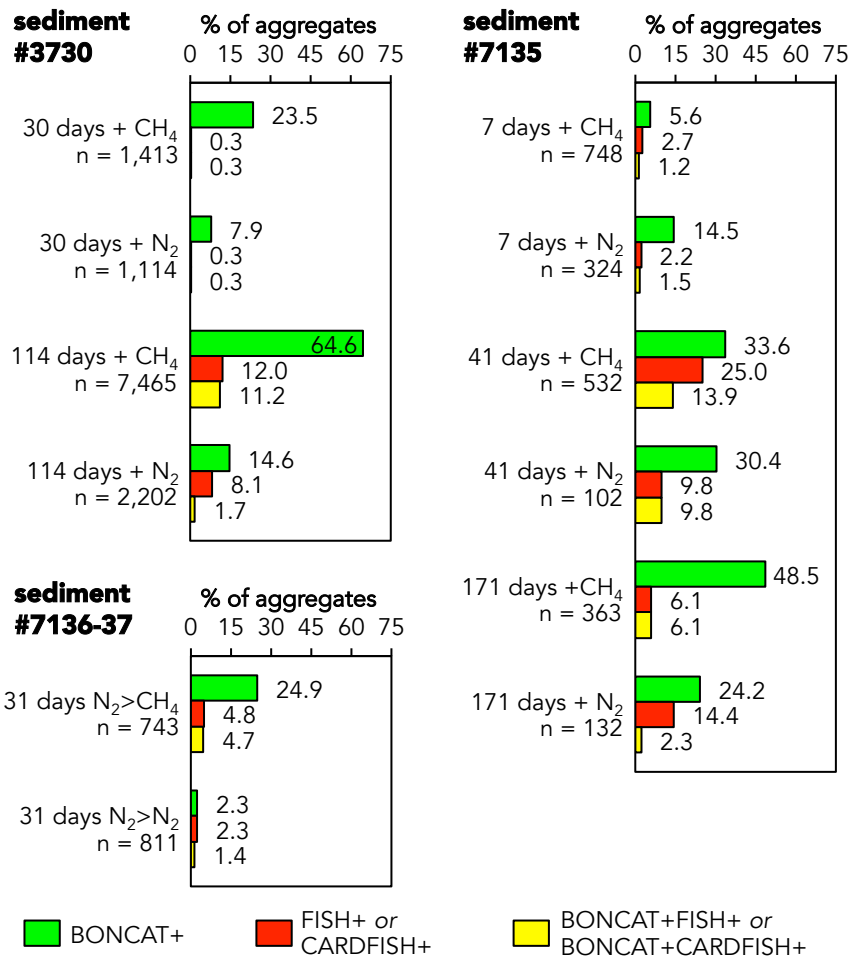


Figure 2

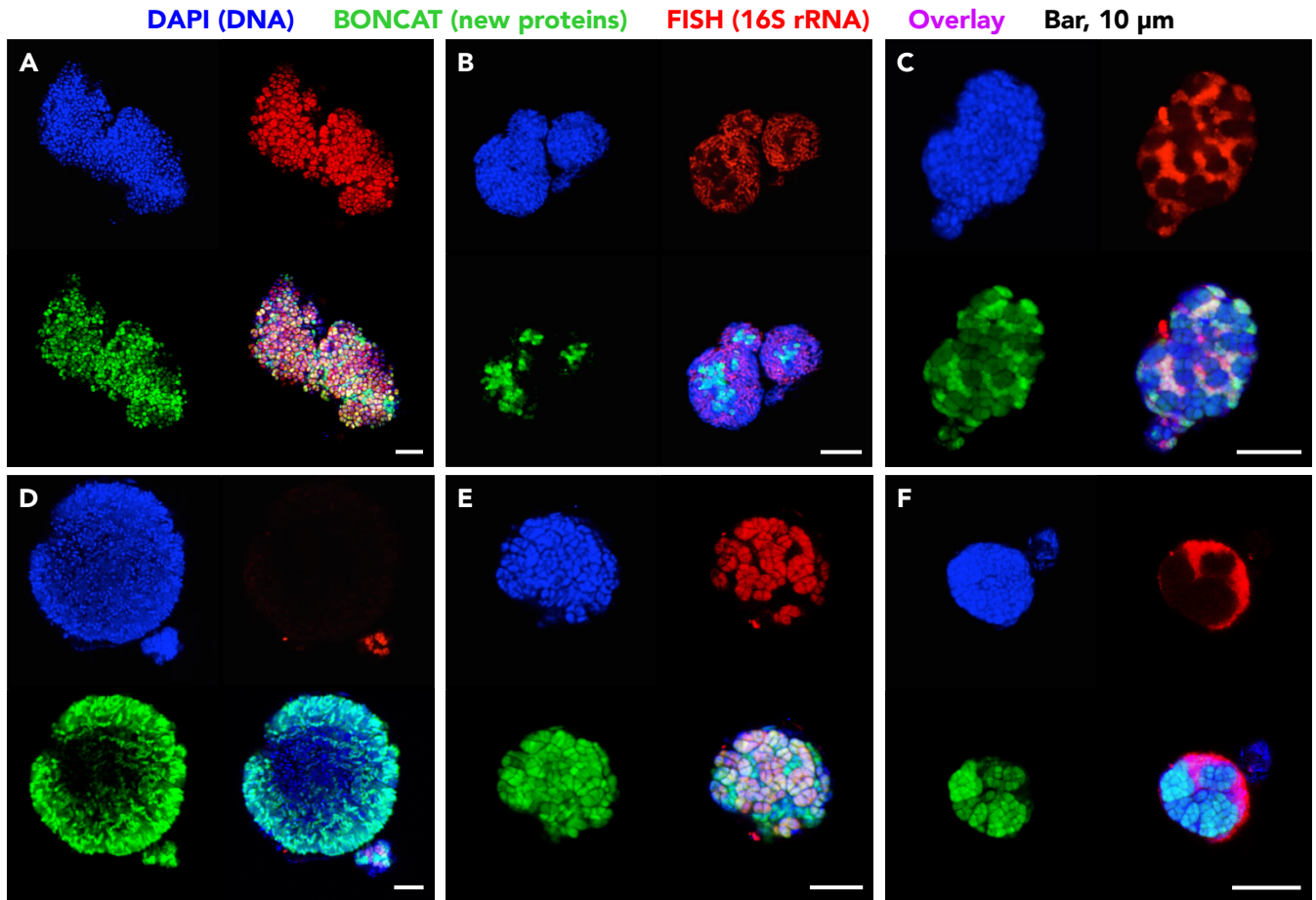


Figure 3

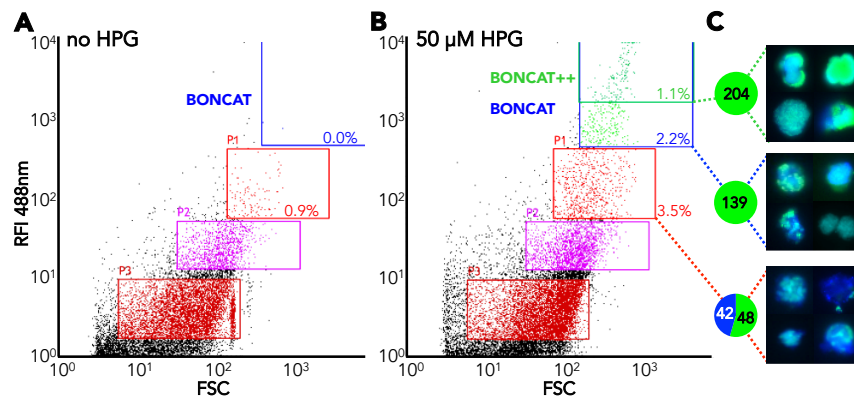
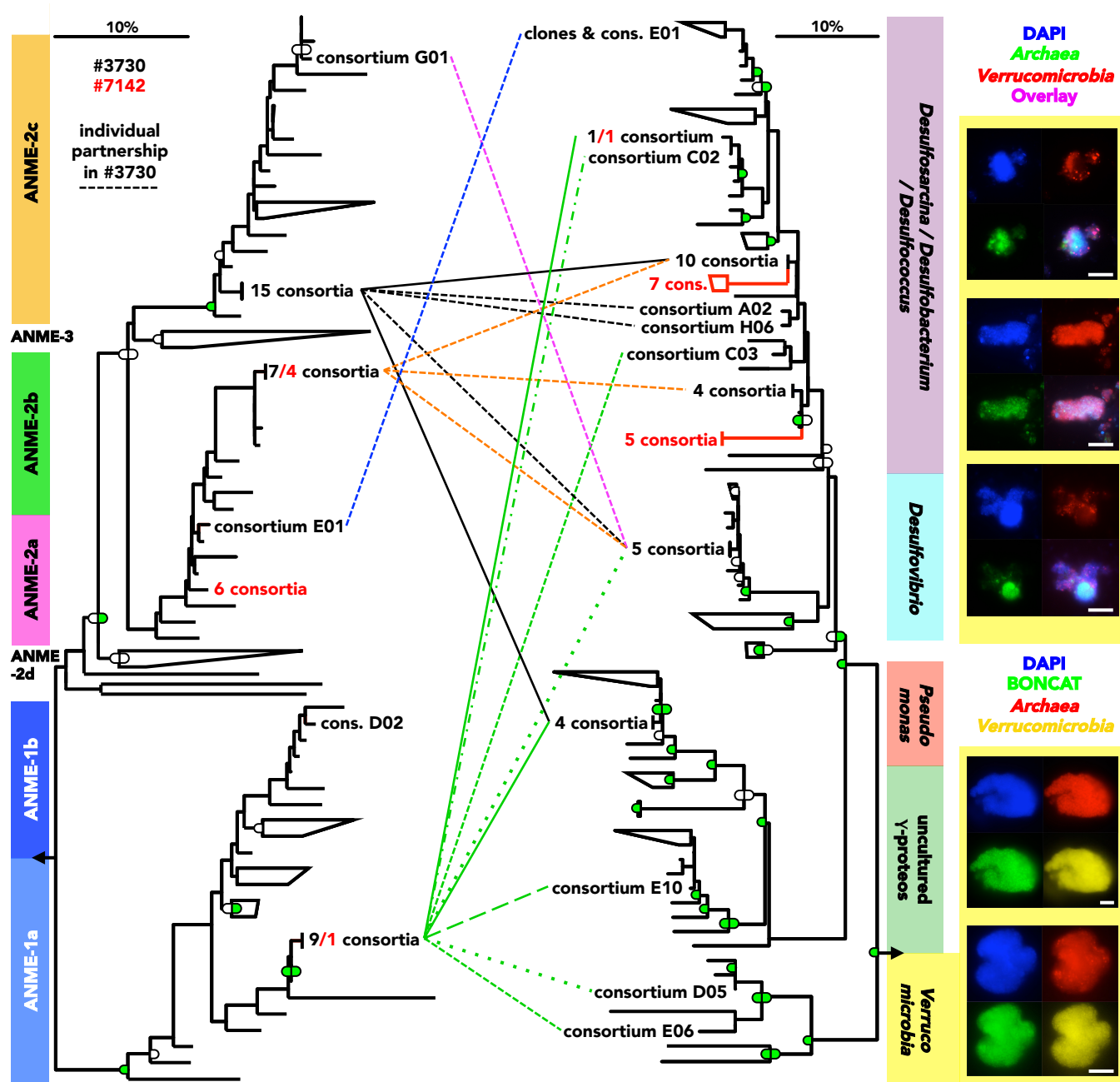


Figure 4

Figure 5



1 *SI Appendix*

2
3 **Visualizing *in situ* translational activity for identifying and sorting slow-**
4 **growing archaeal-bacterial consortia**

5
6 Roland Hatzenpichler^{a,1}, Stephanie A. Connon^a, Danielle Goudeau^b, Rex R. Malmstrom^b, Tanja
7 Woyke^b, Victoria J. Orphan^{a,1}

8
9 ^a Division of Geological and Planetary Sciences, California Institute of Technology, Pasadena,
10 CA-91125, USA

11 ^b Department of Energy Joint Genome Institute, Walnut Creek, CA-94598, USA

12 ¹ Address correspondence to hatzenpichler@caltech.edu and vorphan@gps.caltech.edu

15 **SI Appendix Results and Discussion**

16 **Factors limiting the absolute quantification of newly synthesized proteins.** BONCAT has
17 the theoretical potential to detect all *de novo* synthesized proteins that contain at least one Met,
18 *i.e.* >99% of proteins in an average archaeal and bacterial proteome. However, in practice several
19 factors reduce this sensitivity and prohibit the absolute quantification of the amount of new
20 protein, and, in consequence, of cell doubling times, from fluorescence data. (i) the process(es)
21 by which HPG enters the cell is currently unknown and might depend on the physiological state
22 of the cell or differ between different taxonomic groups; (ii) the rate at which HPG substitutes
23 Met during protein synthesis has so far only been studied for *E. coli* (1) and might deviate in
24 other organisms; (iii) due to varying contents of Met and contrasting copy numbers of proteins,
25 distinct peptides contribute differently to overall fluorescence; and (iv) the extent by which
26 protein-recycling and post-translational modification affect the stability of HPG (in particular its
27 alkyne group) is currently unknown.

28 **CARD-FISH vs. FISH.** Our CARD-FISH experiments revealed marked discrepancies in the
29 efficiencies to permeabilize and fluorescently detect different ANME-subgroups. Most
30 importantly, while ANME-1 constituted only 0.6% of all taxonomically identified consortia in
31 our FISH experiments on sample #3730 (114 days sample; n=167 consortia), the same sub-group
32 represented 81.3% of detected ANME-consortia in our CARD-FISH dataset (n=48) (Tab. 1).
33 This result is mainly explained by the inability of the employed CARD-FISH protocol to detect
34 ANME-2a and -2c consortia in our samples. This finding is in contrast to two recent studies that
35 employed near-identical permeabilization protocols for the successful visualization of these
36 ANME-groups in other methane seep sediments (2, 3).

37 **Comparing ANME-community structure in sediment #3730 to previous studies.** The
38 very low proportion of aggregated ANME-1 in our Hydrate Ridge sediment (#3730) is consistent
39 with a previous study on this methane seep, that found ANME-1 occurred mostly as planktonic
40 cells rather than in multicellular associations (4, 5). Because of our focus on syntrophic consortia
41 in this study, we initially separated microbial aggregates >3 μm from sediment particles.
42 Planktonic ANME-1 cells thus might have partly evaded FISH-detection. It should however be
43 noted, that our filtered samples contained large numbers of individual cells and that in no #3730
44 sample individual cells were found to bind the ANME-1-specific probe.

45 ANME-2a and -2c probes used in this study have been successfully employed in previous
46 mono-FISH studies of geographically distinct Hydrate Ridge sediment samples with
47 hybridization rates of 20-80% of all DAPI-stained AOM-consortia (5, 6). Because of the high
48 spatial variance in ANME-community structure (5, 7) it is, however, possible that our specific
49 sediment samples hosted a unique combination of ANME-clades. Alternatively, ANME-
50 community structure might have diverged from its original composition during the nearly four
51 years of incubation in the lab before the experiments described herein were conducted.

52 **Considerations on the environmental application of BONCAT.** In contrast to the well-
53 established stable isotope probing approach, the universal applicability of BONCAT is currently
54 untested and several questions demand rigorous investigation in future studies: (i) the

55 mechanism(s) by which bioorthogonal amino acids are taken up by cells is currently unknown. If
56 active transporters are required for their uptake, their absence would prohibit the application of
57 BONCAT to that particular cell. To that effect, the recent report of up to 100% BONCAT-
58 labeling efficiency of planktonic microbes in surface seawater is encouraging (8). (ii) HPG and
59 AHA, the bioorthogonal amino acids that have been used in environmental studies so far (8, and
60 this study, 9), have to compete with intracellular Met for incorporation into newly being made
61 proteins. The preference of the translational machinery for Met over its synthetic surrogates (1)
62 might therefore restrict the use of BONCAT in habitats featuring high concentrations of free
63 Met. (iii) Lastly, substituting proteins with synthetic amino acids bears a high risk of interfering
64 with the cellular machinery. We recently demonstrated that the addition of up to 1 mM of HPG
65 or AHA had no detectable effect on the growth of several different, physiologically distinct
66 archaeal and bacterial pure cultures for at least one cell generation. At longer incubation times,
67 however, inhibition of growth could be observed at these high concentrations (9, 10, and
68 Hatzenpichler, unpubl.). For environmental applications we thus recommend that low
69 concentrations of bioorthogonal amino acid should be employed, incubation times kept to a
70 minimum, and complementary experiments testing for potential community shifts be performed
71 (for details see 10).
72

73 **SI Appendix Material and Methods**

74 **Environmental sampling and storage.** Sediment sample #3730 was obtained from Hydrate
75 Ridge South methane seep field (Atlantis cruise AT-15-68, Alvin Dive 4635; push-core 16;
76 44°34.09 N, 125°9.14 W; 775 m water depth; sediment horizon 0-6 cm; 4°C *in situ* temperature)
77 on August 7th 2010. Sediment was stored under argon headspace in a Mylar bag for five weeks,
78 before being transferred to a 1 L glass bottle with a 1.38 bar 100% CH₄ headspace, which was
79 stored at 4°C. Seawater and headspace were exchanged in regular intervals to prevent the
80 accumulation of inhibitory compounds.

81 Sediment samples #7135 and #7136-37/37 were collected from Santa Monica basin on May
82 9th 2013 (R/V Western Flyer MBARI Cruise 2013; dive 463; push-core 43; 33°47.34 N,
83 118°40.10 W; 860 m water depth; horizons 6-9 cm (#7135) and 9-15/15-22 cm (#7136-37/37,
84 pooled) below a pink and white microbial mat; 4°C) . Sediment slurry were stored in a glass
85 bottle for ~1 year under argon at 4°C, before the experiments described below were carried out.

86 Sediment sample #7142 was collected from Santa Monica basin on May 7th 2013 (R/V
87 Western Flyer MBARI Cruise 2013; dive 459; push-core 74; 35°47.34 N, 118°40.09 W; 863 m
88 depth; sediment horizon 4-6 cm; 4°C *in situ* temperature). The sediment was sealed under argon
89 and stored at 4°C. After 40 days of storage, the sediment was suspended in anaerobic natural
90 bottom seawater from the site in an anaerobic chamber (3% H₂ in N₂) and aliquots were over-
91 pressured with 1.5 bar CH₄. The sediment was kept for 12 months under 1.5 bar 100% CH₄ in
92 natural bottom seawater that was exchanged every three months.

93 Sediment sample #5119 was collected from the Hydrate Ridge methane field during Atlantis
94 Cruise AT-18-10 on September 1st 2011. (44°40.02 N, 125°6.00 W; dive J2-593 E4A; push-core
95 36 through a yellow microbial mat; water depth 600 m; sediment horizon 9-12 cm). Sediment
96 #5202 was collected during the same cruise on September 3rd 2011, dive J2-593 E6B (44°40.02
97 N, 125°7.51 W; push-core 18 through a pink-white microbial mat; water depth 601 m; horizon 3-
98 6 cm;).

99 Carbonate #3439 was collected from atop an active seep at the Hydrate Ridge methane field
100 during cruise AT-15-68 on August 1st, 2010 (44°34.09 N, 125°9.14 W; dive AD4629; water
101 depth 775 m). Carbonate sample #2450 was retrieved from sediment sample #2450 collected at
102 Eel River Basin on July 27th 2005 (40°48.68 124°36.73 W; dive T-864; push-core 49; horizon 0-
103 2 cm; water depth 516 m).

104 Information on the geochemical characteristics of the sampling sites may be requested from
105 the corresponding authors.

106 **Setup of incubations.** All samples were kept in an ice bath at all times during handling.
107 Artificial sea-water (ASW) consisted of 10.9 g MgCl₂ 6H₂O, 0.2 g NaHCO₃, 0.76 g KCl, 25.9 g
108 NaCl, 1.47 g CaCl₂ 2H₂O, 3.98 g Na₂SO₄, and 26.73 mg NH₄Cl L⁻¹ ddH₂O at pH 7.4. 1 mL
109 vitamin solution (see medium 141, www.dsmz.de) and 1 mL trace element solution SL-10 (see
110 www.dsmz.de) were also added. Before use, ASW was filtered through a 0.2 µm filter and N₂-
111 bubbled for 10 minutes. ASW was kept on ice during handling.

112 ~50 ml of wet sediment #3730 were re-suspended in ASW, yielding a total volume of ~130
113 mL. 20 mL aliquots of homogenized slurry were transferred into 160 mL serum bottles and 30
114 mL of ASW were added. Bottles were sealed with rubber stoppers, headspaces flushed with
115 either 100% CH₄ or 100% N₂ for 5 min before being pressurized with 2 bar 100% CH₄ or 100%
116 N₂. Sediment was allowed to equilibrate over-night (~18 h) at 4°C in the dark. 0.2 µm-filtered *L*-
117 homopropargylglycine (HPG; Click Chemistry Tools) in ddH₂O was added to reach a final
118 concentration of 50 µM. Control incubations without HPG were supplemented with sterile
119 ddH₂O to reach equal volumes. All bottles were then flushed for 5 min, pressurized with 2 bar
120 CH₄ or N₂, and incubated in the dark at 4°. In total, 6 incubations were performed: 2x without
121 HPG plus CH₄; 2x 50 µM HPG plus CH₄; and 2x 50 µM HPG plus N₂.

122 ~100 mL of wet sediment #7135 were re-suspended in ASW, yielding a total volume of ~300
123 mL, and incubated for 15 days under 2 bar 100% CH₄. After this pre-incubation, 100 mL of
124 ASW were added and the slurry homogenized. Under constant N₂-flushing, 35 mL aliquots were
125 transferred into 160 mL serum bottles, bottles sealed with rubber stoppers, and headspaces
126 flushed for 5 min with either 100% CH₄ or 100% N₂, depending on incubation setup. HPG was
127 added to reach a final concentration of either 5 or 50 µM. In addition, controls without HPG
128 were supplemented with sterile ddH₂O to reach equal incubation volumes. Then, all bottles were
129 flushed for 5 min, over-pressurized with 2 bar CH₄ or N₂, and incubated in the dark at 4°C. In
130 total, 12 incubations were performed: 4x without HPG plus CH₄; 4x 50 µM HPG plus CH₄; 2x
131 50 µM HPG plus N₂; and 2x 5 µM HPG plus CH₄.

132 20 mL of wet sediment #7136-37 were re-suspended in ASW, yielding a total volume of ~50
133 mL. The slurry was bubbled with N₂ for 10 min (this was repeated after 5 days), before the bottle
134 was incubated for 124 days under 2 bar N₂ (detectable but non-quantifiable amount of CH₄, 1-10
135 ppm). After this pre-starving, 10 mL aliquots were transferred into 75 mL bottles. HPG was
136 added to reach a final concentration of 50 µM and 2 bar 100% CH₄ or 100% N₂ (2 bar) were
137 added to the headspace of 2 aliquots each. In addition, a control mesocosm was incubated
138 without HPG under 100% CH₄ (2 bar). All bottles were incubated at 4°C in the dark for 31 days.

139 1 mL aliquots of wet sediment #7142 in 5 mL ASW containing 25 mM HEPES buffer (pH
140 7.5), 5 mM sulfide, and 5 mM dissolved inorganic carbon were re-suspended in serum vials,
141 which were then sealed with rubber stoppers (12.9 mL final volume). The headspace was flushed
142 with ¹²CH₄ before 1.0 mL ¹³CH₄ (99% ¹³C, containing 0.05 vol% ¹³CO₂ as impurity; Cambridge
143 Isotope Laboratories) was added. After ~5 days of pre-incubation, HPG was added to two of the
144 four bottles to reach a concentration of 50 µM. In addition, one incubation was performed at 250
145 µM HPG for 25 days and later used for activity-based cell-sorting.

146 **Sampling for molecular and geochemical analyses.** Sampling of sediment microcosms was
147 undertaken at incubation start as well as after 30, 73, and 114 days and 7, 14, 41, 56, and 171
148 days for sediment #3730 and #7135, respectively. Samples for molecular, cellular, and
149 geochemical analyses were removed using sterile syringes while the incubation bottles were kept
150 in an ice bath.

151 At each sampling-point, 0.25 mL of sediment slurry were transferred into a sterile 1.5 mL
152 tube and centrifuged at 16,100 g for 10 sec at room temperature (RT). The supernatant (SN) was
153 removed, mixed in a 1:1 ratio with 0.5 M Zn-Acetate solution and stored for later sulfide
154 analysis. The pellet was flash-frozen using liquid N₂ and stored at -20°C for DNA extraction.
155 0.25 mL of sediment slurry were removed, centrifuged as described above, the SN wasted, and
156 the pellet re-suspended in a 1:1 mix of 1x PBS and absolute ethanol (EtOH). Another 0.25 mL
157 were processed in the same way, but re-suspended in 3% paraformaldehyde (PFA; Electron
158 Microscopy Sciences) in 1x PBS and incubated for 1 h at RT for chemical fixation of cells.
159 Afterwards, biomass was harvested by centrifugation, the SN wasted, and the pellet washed with
160 1.5 mL of 1x PBS. Finally, sediment was centrifuged, the SN wasted, and the biomass re-
161 suspended in a 1:1 mix of 1x PBS and EtOH. All EtOH- or PFA-fixed samples were kept at -
162 20°C until further processing. After sampling (30, 73, and 114 days and 7, 14, 41, 56, and 171
163 days for #3730 and #7135, respectively), the headspace of bottles was flushed for 3 min with
164 either CH₄ or N₂ before the sediment was again incubated at 4°C with 2 bar of either 100% CH₄
165 or 100% N₂, depending on incubation setup. In addition, after 73 days (#3730) and 41 and 130
166 days (#7135) ~90% of artificial seawater overlying sediment was exchanged. The slurry volume
167 and sediment-to-water ratio of all incubations was identical at all times for each sediment type
168 (#3730 or #7135, respectively). When appropriate, newly added seawater was then supplemented
169 with 5 or 50 µM (final) HPG.

170 **Geochemical analyses.** Sulfide (H₂S plus HS⁻) concentrations were determined via the cline
171 assay (11). Samples were analyzed for statistically relevant differences via student's t-test.
172 Differences were considered to be significant at p≤0.05. Methane oxidation rates for sediment
173 #7142 were determined as described by Scheller *et al.* (12) by measuring the formation of ¹³C-
174 dissolved inorganic carbon (DI¹³C) from ¹³CH₄ over time. Succinctly, 0.25 mL of ASW
175 overlying settled sediment was removed and centrifuged (16,000 g for 5 min). The SN was
176 transferred into 0.6 mL tubes, flash frozen in N₂, and stored at -20 °C until further processing.
177 150 µL of thawed SN was then added to He-flushed vials containing 100 µL H₃PO₄ (85%). The
178 resulting CO₂ was analyzed for isotopic enrichment on a GC-IR-MS GasBench II (Thermo
179 Scientific).

180 **Extraction of microbial aggregates.** To separate microbial aggregations and individual cells
181 from sediment particles, 50 µL of sediment slurry were re-suspended in 450 µL of 1x PBS in a 2
182 mL tube. This solution was chilled in an ice-bath for 15 min before being sonicated 3x for 10 sec
183 at 3-6 W output using a Branson Sonifier 150 (Branson Ultrasonics Corporation). Between
184 pulsing intervals the sample was allowed to cool for 10-30 sec. After sonication, the sample was
185 applied atop of 500 µL Percoll (Sigma-Aldrich) and centrifuged at 16,100 g for 20 min at 4°C.
186 To remove Percoll particles and the majority of individual planktonic cells, the entire SN was re-
187 suspended in 15 mL 1x PBS and filtered through a 3 µm TSTP white polycarbonate filter (EMD
188 Millipore) using a filter tower at ~0.3 bar under-pressure. Each filter was washed with a total
189 volume of 50 mL 1x PBS without letting the filter run dry. Then, particles and biomass that had
190 been retained by the filter were transferred into a 2 mL tube using 1x PBS by repeatedly and

191 vigorously pipetting up-and-down using a 1 mL pipette. DAPI-staining confirmed that this
192 protocol leads to the near-complete transfer of microbial aggregates from the filter into solution
193 (99-100% of DAPI-stained consortia), without selecting for or against a particular type of
194 consortium morphology or size (not shown). After transfer into 1x PBS, biomass was harvested
195 via centrifugation (16,100 g, RT), re-suspended in either 1x PBS (for ‘nonfixed’ BONCAT
196 analyses) or a 1:1 ratio of 1x PBS and EtOH (fixed biomass), and stored at either 4°C (nonfixed)
197 or -20°C (fixed).

198 **List of oligonucleotide probes for FISH and CARD-FISH.** In FISH-experiments
199 combination of mono- and dual-labeled (indicated with ** in the list below) probes were used in
200 different combinations (see Tab. S2): Arch915, specific for most members of the domain
201 *Archaea* (13), used at 35% formamide (FA); EUB338, -II, and -III (*a.k.a.* EUB338mix), which
202 together cover most of the known bacterial diversity (14, 15), used at 35% FA; EUB338-III,
203 specific for most members of the *Verrucomicrobia* (15), used at 35% FA, in combination with
204 EUB338-I and -II as competitor probes; Delta495a** together with its competitor probe, specific
205 for most delta-proteobacteria (16), used at 35% FA; Gam42a, together with its competitor,
206 specific for most gamma-proteobacteria (17), used at 35% FA; Ver47**, specific for
207 *Verrucomicrobia* (18) together with its helper probe H64 (19) at 15% FA; as well as ANME-1-
208 350 (4) (40% FA), ANME-2-932 (*a.k.a.* EelMS-932; 4) (40% FA), ANME-2a-647 (50% FA)
209 (5), and ANME-2c-760** (60% FA) (5), specific for different subpopulations of anaerobic
210 methane-oxidizing euryarchaeotes. In addition, a new probe, ANME-2b-729, was designed,
211 which detects >93% of all ANME-2b-affiliated 16S rRNA sequences in online and lab-internal
212 databases. The new probe has at least 2 mismatches to all other archaeal or bacterial 16S rRNA
213 sequences (tested using probeCheck, ref. 20). After careful evaluation, ANME-2b-729 was used
214 at 20% formamide concentration. Note that this probe has a one-nucleotide overlap with probe
215 ANME-2-712 (5) and should thus not be used in conjunction with this probe. Hybridizations
216 without probe addition or probe NONEUB388 (21) were used as negative controls.

217 With the exception of probe ANME-2a-647, which was used at 40% FA (rather than 50%),
218 all probes employed in CARD-FISH were used at the same FA concentrations as in FISH-
219 experiments. For CARD-FISH, hybridizations with probe NONEUB388 were used as negative
220 controls.

221 **Multiple displacement amplification.** Individual sorted consortia were lysed and subjected
222 to whole genome amplification (WGA) as previously described (22) with the following
223 modifications: WGA was performed with a REPLI-g Single Cell Kit (Qiagen) with a scaled-
224 down reaction volume of 2 µl and DNA-dye SYTO-13 added at 1x for real-time tracking. The
225 cell lysis procedure followed a recently described protocol (22), which was modified by
226 lysozyme treatment. This step included a 15 min RT incubation with 300 nl of 50 U/µl
227 ReadyLyse lysozyme (Epicentre R1810M), which was followed by the addition of 50 nl
228 concentrated DLB buffer (22). Lysis and stop reagents were UV-treated as described (22), while
229 the Master Mix was used as obtained from the manufacturer (Qiagen). The amplification reaction
230 was incubated for 6 hours at 30°C.

231 **16S rRNA gene tag sequencing.** Sediment DNA was extracted using the Power Soil DNA
232 Isolation Kit according to the manufacturer's protocol (MoBio, Carlsbad, CA) and diluted DNA
233 from genome-amplified sorted consortia was used directly. The V4 region of the 16S rRNA gene
234 was amplified from each extract using archaeal and bacterial primers 515F
235 (GTGCCAGCMGCCGCGGTAA) and 806R (GGACTACHVGGGTWTCTAAT) (23, 24).
236 Sediment samples were amplified in duplicate. The non-barcoded primers were used with Q5
237 Hot Start High-Fidelity 2x Master Mix (New England Biolabs, Ipswich, MA) according to the
238 manufacturer's directions using annealing conditions of 54°C for 30 cycles and 58°C for 32
239 cycles for sediments and MDAs, respectively. Duplicates of sediment sample amplifications
240 were then pooled. The barcoded 806R primer (CAAGCAGAAGACGGCATAACGAGAT
241 XXXXXXXXXXXX AGTCAGTCAG CC GGACTACHVGGGTWTCTAAT) was paired with
242 515F in a reconditioning reaction (same conditions as above except for 5 cycles of PCR) to
243 barcode the PCR products. Samples were mixed together in equimolar amounts and purified in
244 bulk through a Qiagen PCR purification kit before submission to Laragen (Culver City, CA) for
245 analysis on an Illumina MiSeq platform. The resulting paired-end sequence data, 2x 250 base
246 pairs (bp), was de-multiplexed and sequences with >1 bp mismatch on the 12 bp barcode were
247 removed. The resulting sequences were passed through Illumina's MiSeq Recorder software to
248 assign quality scores to each base call and remove adapter, barcode and primer sequence.

249 **Analysis of 16S rRNA gene tag sequences.** Sequence data was processed in QIIME version
250 1.8.0 (25) following a recently published protocol (26). Raw sequence pairs were joined and
251 quality-trimmed using the default parameters in QIIME. Sequences were clustered into *de novo*
252 operational taxonomic units (OTUs) with 99% similarity using UCLUST open reference
253 clustering protocol (27). Then, the most abundant sequence was chosen as representative for
254 each *de novo* OTU (28). Taxonomic identification for each representative sequence was assigned
255 using the Silva-115 database (29, 30) clustered at 99% similarity. This SILVA database had been
256 appended with 1,197 in-house high-quality, methane-seep derived bacterial and archaeal clones.
257 Any sequences with pintail values >75 were removed. The modified SILVA database is available
258 upon request from the corresponding authors. OTUs were then filtered to remove singletons from
259 the combined MDA dataset. A threshold filter was used to remove any OTU that occurred below
260 0.01% of the entire combined sediment samples dataset. Known contaminants in PCR reagents
261 as determined by the analysis of negative and positive controls run with each MiSeq set were
262 also removed (31). For the sediment samples, the sequence data was rarified by random
263 subsampling to equal the sample with the least amount of sequence data, resulting in 12,115 and
264 3,707 sequences per sample for sediments #3730 and #7135, respectively. Tables of both
265 absolute and relative abundance were generated at the family level for each sample. For
266 statistical and similarity percentage analyses (Non-metric Multi Dimensional Scaling (NMDS),
267 Analysis of Similarity (ANOSIM), and Similarity Percentage (SIMPER)), family level
268 abundance tables were square-root transformed prior to generation of Bray Curtis similarity
269 matrices and analyzed using Primer-E software (<http://www.primer-e.com>). Differences were
270 considered to be significant at $p \leq 0.05$.

271 **Phylogenetic analysis.** 16S rRNA gene tag sequences from each consortium as well as
272 closely related sequences from online databases (identified via the BLAST-algorithm of NCBI)
273 were imported into and analyzed via the ARB software package (32). Sequences were
274 automatically aligned to reference sequences of all ANME-subpopulations as well as relevant
275 bacterial clades contained within the SILVA-115 database that had been amended with 1,197 in-
276 house seep derived clones. Sequences from cultured representatives of archaeal phyla *Thaum-*
277 and *Euryarchaeota* were used as outgroup for reconstruction of the archaeal tree. Members of
278 the *Planctomycetes* were chosen as outgroup for the bacterial tree. Both alignments were
279 manually curated and termini-filters were created. During the phylogenetic reconstruction of
280 archaeal (all >1,100 nt in length) and bacterial (all >1,000 nt in length) sequences, 958 and 1,255
281 positions were considered, respectively. Phylogenies were modeled using RaxML and short tag-
282 sequences were individually added to the tree using the parsimony interactive tool in ARB
283 without changing the overall topology of the tree. In addition, maximum parsimony (100x
284 replications) and Neighbor Joining (1,000x replications) trees were calculated and bootstrap
285 values projected onto the RaxML tree.

286

287

288 SI Appendix Figure and Table Legends

289 **Fig. S1.** Sediment sulfide production rates and methane oxidation rates are not affected by
290 the presence of HPG. (A) Sulfide [$\text{H}_2\text{S} + \text{HS}^-$] levels cannot be directly compared between
291 different time-points, because seawater and headspace of incubations were refreshed in regular
292 intervals. In contrast to HPG, CH_4 has a statistically significant effect on sulfide production
293 ($p=0.0183$ and $p=0.0063$ for #3730 and #7135 after 114 and 56 days of incubation, respectively).
294 Sulfide levels in sediment #7135 samples #09 and #10 (both without CH_4) were below detection
295 limit (bd) after 171 days of incubation. (B) Sediment methane oxidation rates are not affected by
296 the presence of HPG over a course of up to 25 days. Four separate aliquots of sediment #7142
297 were incubated in the absence of HPG for ~ 5 days, after which $50 \mu\text{M}$ HPG (final concentration)
298 were added to two incubations. Note that one of the HPG-containing incubations exhibited low
299 rates of AOM from the start of the experiment on. Because of this, the experiment was stopped
300 after ~ 10 days of incubation. Compilations of representative AOM-consortia from the end-points
301 of two incubations are shown on the right. Green fluorescence indicates that cells have been
302 translationally active during time of incubation. DAPI-stained of DNA is in blue. Methane
303 oxidation rates were measured as ^{13}C -dissolved inorganic carbon [DIC] formed from $^{13}\text{CH}_4$.
304 Sampling on day 5 was performed immediately after addition of HPG.

305
306 **Fig. S2.** Bray Curtis similarity indexes of the microbial communities of sediments #3730 (A)
307 and #7135 (B) after incubation in the absence or presence of HPG for 114 and 171 days,
308 respectively. For statistical analyses see Fig. S3 and S4.

309
310 **Fig. S3.** Non-metric Multidimensional Scaling (NMDS) ordinations of 16S rRNA gene tag
311 sequences demonstrated that neither HPG (A) nor CH_4 (B) have a statistically relevant effect on
312 the microbial community of sediment #3730 after 114 days of incubation. Stress values of
313 NMDS-ordinations and p-values of concomitant Anosim analyses for whole communities and
314 ANME-SRB-related lineages specifically are shown next to the plots. n, number of sequences
315 per sample. The more similar microbial communities from two samples are, the closer they lie
316 together. Differences between samples were considered to be significant at $p \leq 0.05$.

317
318 **Fig. S4.** Non-metric Multidimensional Scaling (NMDS) ordinations of 16S rRNA gene tag
319 sequences demonstrated that HPG (A) does not have a statistically relevant effect on the
320 microbial community of sediment #7135 after 171 days of incubation. (B) The absence of CH_4 ,
321 on the other hand, has a clear effect on the community composition. Stress values of NMDS-
322 ordinations and p-values of concomitant Anosim analyses for whole communities and ANME-
323 SRB-related lineages specifically are shown next to the plots. Dotted lines connect the individual
324 sampling points for each incubation bottle. n, number of sequences per sample. The more similar
325 microbial communities from two samples are, the closer they lie together. Differences between
326 samples were considered to be significant at $p \leq 0.05$.

327

328 **Fig. S5.** Relative abundances of ANME-related archaea and sulfate-reducing bacteria in
329 sediment #3730 (A) or #7135 (B) over time. Abundance-based color-coding indicates relative
330 abundance of taxa within a sample. Sequences summarized as “other archaea”, which are slightly
331 enriched in #7135 samples incubated in the absence of CH₄, were related to rRNA genes from
332 Marine Benthic Group D / Deep Sea Hydrothermal Vent Euryarchaeotal Group 1 as well as the
333 Marine Hydrothermal Vent Group and Miscellaneous Euryarchaeotal Group. The physiology of
334 these uncultured, yet environmentally widely distributed clades is currently unknown. However,
335 recent genomic data suggest an implication of members of Marine Benthic Group D in the
336 degradation of detrital proteins in marine sediments (33).

337
338 **Fig. S6.** Extended versions of the phylogenetic trees shown in Fig. 5. Green and white
339 colored boxes show support $\geq 90\%$ and $\geq 70\%$, respectively. Values $< 70\%$ are not shown. Left
340 and right boxes indicate max. parsimony (100x) and neighbor joining (1,000x) values,
341 respectively. Scale bars equal 10% estimated sequence divergence. Numbers in boxes give the
342 number of sequences within a group. 16S rRNA gene tag sequences were added after tree
343 construction without changing overall tree topology. Dotted lines indicate individual partnerships.
344 The scales bars represent 10% estimated sequence divergence.

345
346 **Fig. S7.** Representative images of our FISH-based screening of methane seep sediment and
347 carbonate samples for associations of *Archaea* and members of the *Verrucomicrobia*. Arch915,
348 probe specific for archaea; EUB338-III, a probe specific for most *Verrucomicrobia*; comp,
349 unlabeled competitor probes EUB338-I and II; Ver47, a *Verrucomicrobia*-specific probe, used
350 together with an unlabeled helper probe (helper). For references of FISH-probes and detailed
351 aggregate-counts for specific samples refer to *SI Appendix* and Tab. S3.

352
353 **Tab. S1.** Incubation setup and sampling details. -, not determined; d, days of incubation; Y,
354 yes. 5/50, 5/50 μM of HPG.

355
356 **Tab. S2.** Details on BONCAT-FISH experiments summarized in Fig. 2 and 4. For probe
357 specificities, see Materials and Methods section. comp, competitor probe; nd, not determined; d,
358 days of incubation.

359
360 **Tab. S3.** Details on *Verrucomicrobia*-FISH experiments. For probe specificities, see
361 Materials and Methods section. comp, competitor probe; help, helper probe; cons, consortium.

362

363 **References to *SI Appendix***

- 364 1. Kiick KL, Saxon E, Tirrell DA, Bertozzi CR (2002) Incorporation of azides into
365 recombinant proteins for chemoselective modification by the Staudinger ligation. *Proc Natl*
366 *Acad Sci U S A* 99(1):19-24.
- 367 2. Green-Saxena A, Dekas AE, Dalleska NF, Orphan VJ (2014) Nitrate-based niche
368 differentiation by distinct sulfate-reducing bacteria involved in the anaerobic oxidation of
369 methane. *ISME J* 8(1):150-163.
- 370 3. Trembath-Reichert E, Green-Saxena A, Orphan VJ (2013) Whole cell immunomagnetic
371 enrichment of environmental microbial consortia using rRNA-targeted Magneto-FISH.
372 *Methods Enzymol* 531:21-44.
- 373 4. Boetius A, *et al.* (2000) A marine microbial consortium apparently mediating anaerobic
374 oxidation of methane. *Nature* 407(6804):623-626.
- 375 5. Knittel K, Losekann T, Boetius A, Kort R, Amann R (2005) Diversity and distribution of
376 methanotrophic archaea at cold seeps. *Appl Environ Microbiol* 71(1):467-479.
- 377 6. Nauhaus K, Albrecht M, Elvert M, Boetius A, Widdel F (2007) *In vitro* cell growth of
378 marine archaeal-bacterial consortia during anaerobic oxidation of methane with sulfate.
379 *Environ Microbiol* 9(1):187-196.
- 380 7. Ruff SE, *et al.* (2015) Global dispersion and local diversification of the methane seep
381 microbiome. *Proc Natl Acad Sci U S A* 112(13):4015-4020.
- 382 8. Samo TJ, Smriga S, Malfatti F, Sherwood BP, Azam F (2014) Broad distribution and high
383 proportion of protein synthesis active marine bacteria revealed by click chemistry at the
384 single cell level. *Front Mar Sci* doi: 10.3389/fmars.2014.00048.
- 385 9. Hatzenpichler R, *et al.* (2014) *In situ* visualization of newly synthesized proteins in
386 environmental microbes using amino acid tagging and click chemistry. *Environ Microbiol*
387 16(8):2568-2590.
- 388 10. Hatzenpichler R, Orphan VJ (2015) Detection of protein-synthesizing microorganisms in
389 the environment via bioorthogonal non-canonical amino acid tagging (BONCAT).
390 *Hydrocarbon and Lipid Microbiology Protocols*, ed McGenity TJ (Springer, Berlin
391 Heidelberg), Vol Vol. 7: Single-cell and single-molecule methods.
- 392 11. Cline JD (1969) Spectrophotometric Determination of Hydrogen Sulfide in Natural Waters.
393 *Limnol Oceanogr* 14(3):454-458.
- 394 12. Scheller S, Hang Y, Chadwick GL, McGlynn SE, Orphan VJ (Artificial electron acceptors
395 decouple archaeal methane oxidation from sulfate reduction. *Science* in proof.
- 396 13. Stahl DA, Amann R (1991) Development and application of nucleic acid probes. *Nucleic*
397 *acid techniques in bacterial systematics*, eds Stackebrandt EG & Goodfellow M (John
398 Wiley & Sons Ltd., Chichester, New York), pp 205-248.
- 399 14. Amann RI, *et al.* (1990) Combination of 16S rRNA-targeted oligonucleotide probes with
400 flow cytometry for analyzing mixed microbial populations. *Appl Environ Microbiol*
401 56(6):1919-1925.
- 402 15. Daims H, Bruhl A, Amann R, Schleifer KH, Wagner M (1999) The domain-specific probe
403 EUB338 is insufficient for the detection of all *Bacteria*: development and evaluation of a
404 more comprehensive probe set. *Syst Appl Microbiol* 22(3):434-444.
- 405 16. Lucker S, *et al.* (2007) Improved 16S rRNA-targeted probe set for analysis of sulfate-
406 reducing bacteria by fluorescence in situ hybridization. *J Microbiol Methods* 69(3):523-
407 528.

- 408 17. Manz W, Amann R, Ludwig W, Wagner M, Schleifer KH (1992) Phylogenetic
409 oligodeoxynucleotide probes for the major subclasses of proteobacteria - problems and
410 solutions. *Syst Appl Microbiol* 15(4):593-600.
- 411 18. Arnds J, Knittel K, Buck U, Winkel M, Amann R (2010) Development of a 16S rRNA-
412 targeted probe set for Verrucomicrobia and its application for fluorescence in situ
413 hybridization in a humic lake. *Syst Appl Microbiol* 33(3):139-148.
- 414 19. Bergen B, Herlemann DP, Labrenz M, Jurgens K (2014) Distribution of the
415 verrucomicrobial clade Spartobacteria along a salinity gradient in the Baltic Sea. *Environ*
416 *Microbiol Rep* 6(6):625-630.
- 417 20. Loy A, *et al.* (2008) probeCheck - a central resource for evaluating oligonucleotide probe
418 coverage and specificity. *Environ Microbiol* 10(10):2894-2898.
- 419 21. Wallner G, Amann R, Beisker W (1993) Optimizing fluorescent *in situ* hybridization with
420 rRNA-targeted oligonucleotide probes for flow cytometric identification of
421 microorganisms. *Cytometry* 14(2):136-143.
- 422 22. Rinke C, *et al.* (2014) Obtaining genomes from uncultivated environmental
423 microorganisms using FACS-based single-cell genomics. *Nat Protoc* 9(5):1038-1048.
- 424 23. Caporaso JG, *et al.* (2012) Ultra-high-throughput microbial community analysis on the
425 Illumina HiSeq and MiSeq platforms. *ISME J* 6(8):1621-1624.
- 426 24. Caporaso JG, *et al.* (2011) Global patterns of 16S rRNA diversity at a depth of millions of
427 sequences per sample. *Proc Natl Acad Sci U S A* 108 Suppl 1:4516-4522.
- 428 25. Caporaso JG, *et al.* (2010) QIIME allows analysis of high-throughput community
429 sequencing data. *Nature Methods* 7(5):335-336.
- 430 26. Mason OU, *et al.* (2015) Comparison of Archaeal and Bacterial Diversity in Methane Seep
431 Carbonate Nodules and Host Sediments, Eel River Basin and Hydrate Ridge, USA. *Microb*
432 *Ecol.*
- 433 27. Edgar RC (2010) Search and clustering orders of magnitude faster than BLAST.
434 *Bioinformatics (Oxford, England)* 26(19):2460-2461.
- 435 28. Wang Q, Garrity GM, Tiedje JM, Cole JR (2007) Naive Bayesian classifier for rapid
436 assignment of rRNA sequences into the new bacterial taxonomy. *Applied and*
437 *Environmental Microbiology* 73(16):5261-5267.
- 438 29. Pruesse E, *et al.* (2007) SILVA: a comprehensive online resource for quality checked and
439 aligned ribosomal RNA sequence data compatible with ARB. *Nucleic acids research*
440 35(21):7188-7196.
- 441 30. Quast C, *et al.* (2013) The SILVA ribosomal RNA gene database project: improved data
442 processing and web-based tools. *Nucleic acids research* 41(D1):D590-D596.
- 443 31. Salter SJ, *et al.* (2014) Reagent and laboratory contamination can critically impact
444 sequence-based microbiome analyses. *Bmc Biology* 12.
- 445 32. Ludwig W, *et al.* (2004) ARB: a software environment for sequence data. *Nucleic Acids*
446 *Res* 32(4):1363-1371.
- 447 33. Lloyd KG, *et al.* (2013) Predominant archaea in marine sediments degrade detrital proteins.
448 *Nature* 496(7444):215-218.

449

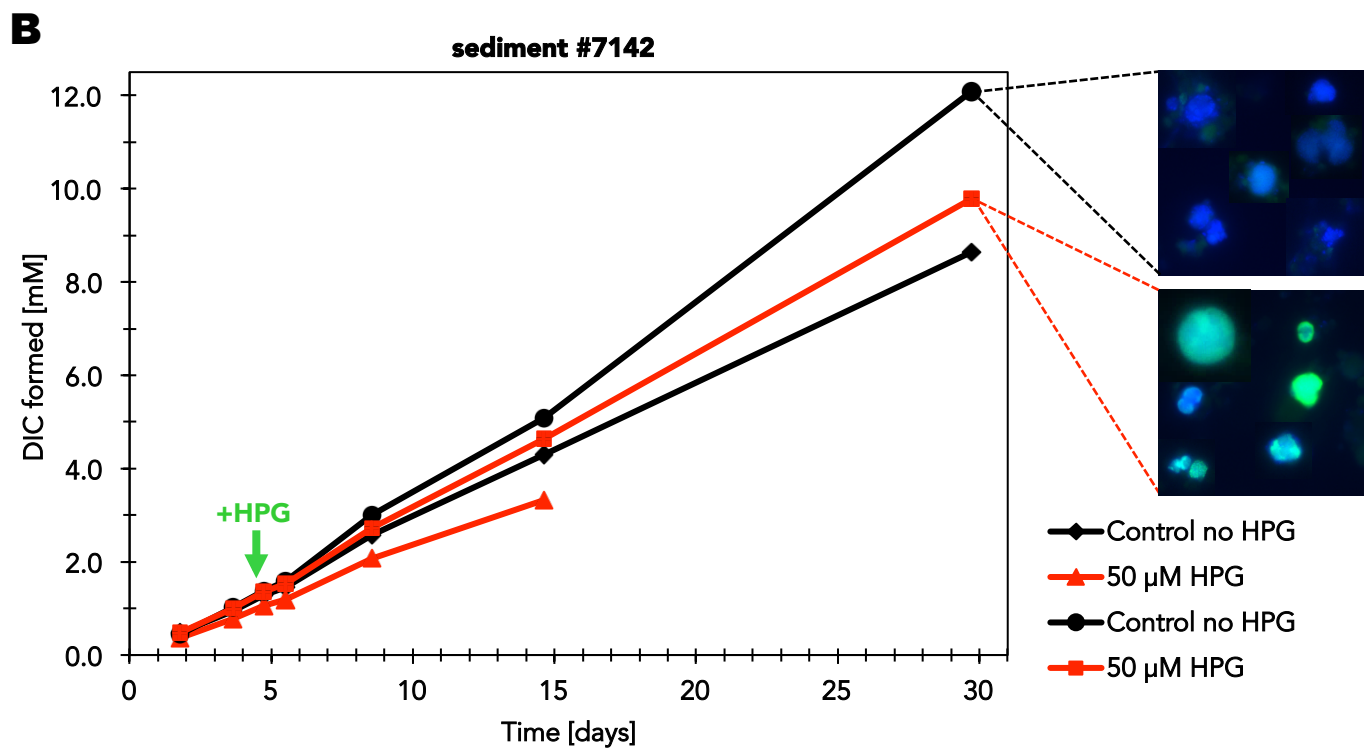
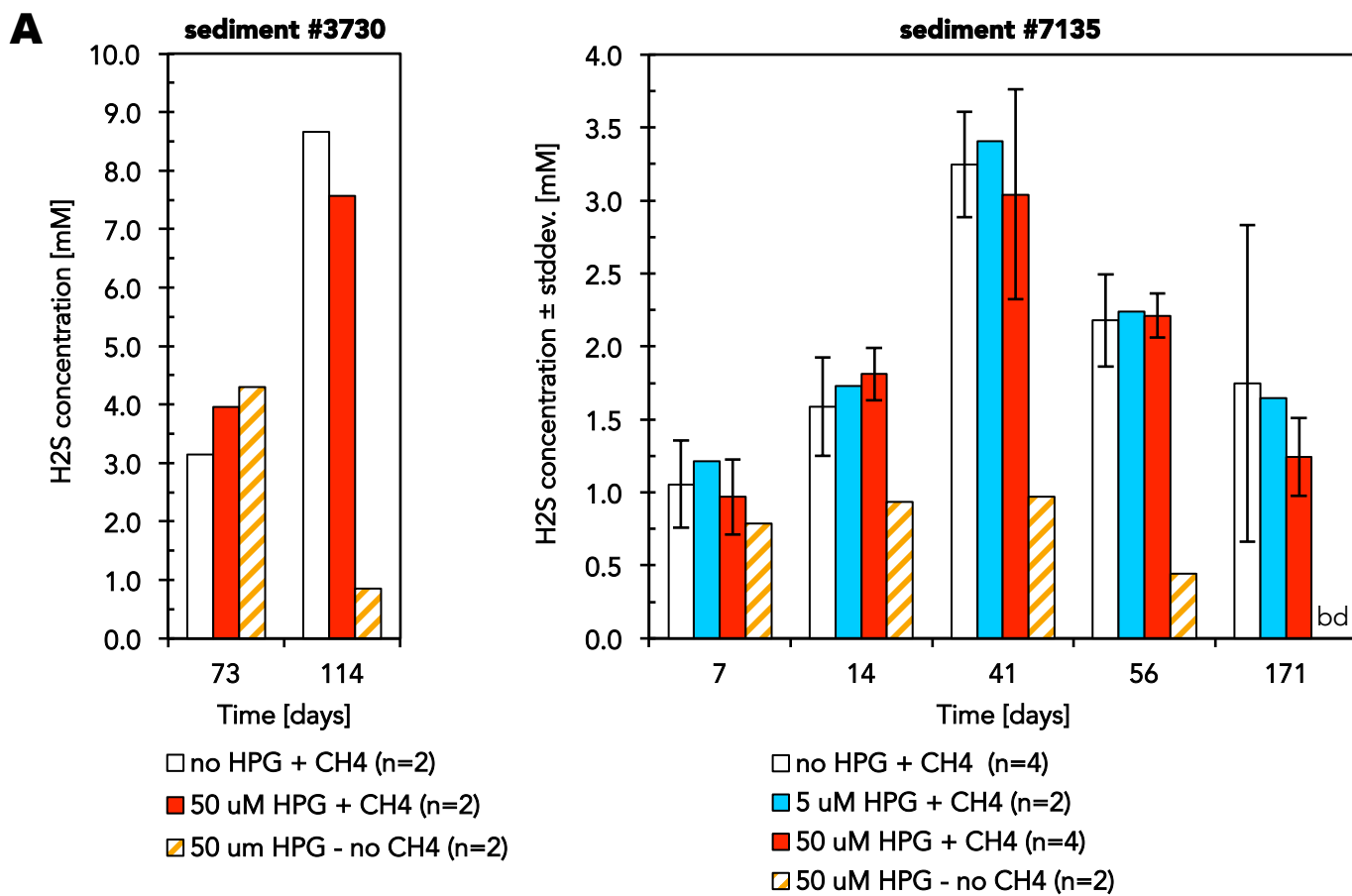


Figure S1

A

3730				HPG	NO	NO	NO	50	50	50	50
				CH4	Y	Y	Y	Y	Y	NO	NO
				Time	0	114	114	114	114	114	114
HPG	CH4	Time	Sample	#0	#1	#2	#3	#4	#5	#6	
NO	Y	0	#0								
NO	Y	114	#1	91.7							
NO	Y	114	#2	92.0	94.5						
50	Y	114	#3	90.8	94.3	94.2					
50	Y	114	#4	91.0	94.4	93.1	94.8				
50	NO	114	#5	88.4	92.6	91.8	93.2	92.2			
50	NO	114	#6	91.1	93.6	92.8	93.6	92.7	92.8		

NO	no HPG addition	HPG
5	5 μM HPG	
50	50 μM HPG	

NO	30 psi N2	CH4
Y	30 psi CH4	

3730: 12,115 sequences
7135: 3,707 sequences

Bray Curtis similarity [%]	
85.7	94.8

0	start	Time
114	114 days	
171	171 days	

B

7135				HPG	NO	NO	NO	NO	NO	NO	NO	NO	NO	NO	NO	NO	NO	NO	NO	NO	NO	NO	NO	5	5	5	5
				CH4	Y	Y	Y	Y	Y	Y	Y	Y	Y	Y	Y	Y	Y	Y	Y	Y	Y	Y	Y	Y	Y	Y	Y
				Time	41	41	41	41	171	171	171	171	171	171	171	171	171	171	171	171	171	171	171	171	171	171	171
HPG	CH4	Time	Sample	#01	#02	#03	#04	#01	#02	#03	#04	#05	#06	#07	#08	#05	#06	#07	#08	#09	#10	#09	#10	#11	#12	#11	#12
NO	Y	41	#01																								
NO	Y	41	#02	92.7																							
NO	Y	41	#03	92.9	92.3																						
NO	Y	41	#04	91.2	91.9	91.8																					
NO	Y	171	#01	87.9	88.2	87.7	88.5																				
NO	Y	171	#02	87.3	87.8	89.0	87.6	86.6																			
NO	Y	171	#03	87.6	88.2	87.7	88.1	91.2	88.9																		
NO	Y	171	#04	87.1	88.2	88.1	87.3	89.9	87.3	90.1																	
50	Y	41	#05	91.8	91.4	92.3	90.7	87.8	88.3	87.2	87.1																
50	Y	41	#06	92.1	92.2	93.7	90.9	87.6	89.2	87.7	87.9	90.7															
50	Y	41	#07	93.4	92.4	92.6	92.3	87.9	87.0	87.6	87.5	91.3	92.8														
50	Y	41	#08	90.9	92.7	92.5	91.7	88.8	88.8	88.5	88.7	91.4	91.5	91.6													
50	Y	171	#05	89.3	88.9	89.2	88.6	89.9	88.0	89.6	88.4	88.5	88.7	89.4	88.4												
50	Y	171	#06	88.8	89.0	89.3	88.5	90.3	87.3	90.8	90.0	87.5	88.8	88.5	88.9	90.7											
50	Y	171	#07	90.0	91.0	90.4	89.4	90.3	87.5	89.7	89.8	89.5	89.5	89.2	89.9	89.7	89.8										
50	Y	171	#08	89.9	90.6	90.5	89.6	89.2	89.8	89.1	88.8	90.9	90.3	90.5	90.4	90.9	89.1	90.1									
50	NO	41	#09	89.9	89.3	90.2	90.4	86.7	85.7	88.6	86.7	89.0	87.9	88.7	90.1	87.4	88.3	89.9	87.4								
50	NO	41	#10	91.3	91.8	92.1	89.8	86.8	89.1	86.4	86.2	90.8	91.6	91.0	91.3	88.1	87.8	89.4	90.7	89.2							
50	NO	171	#09	89.3	89.9	88.8	88.1	89.4	87.7	88.9	88.4	88.1	88.2	88.6	88.3	90.5	89.0	90.5	90.1	88.4	88.5						
50	NO	171	#10	89.2	88.9	89.3	88.2	89.4	86.8	88.8	88.9	88.0	87.7	88.7	89.0	89.0	89.5	91.2	88.5	89.4	88.3	90.4					
5	Y	41	#11	91.0	92.1	91.9	90.8	88.1	88.5	88.2	86.5	90.2	90.6	90.8	91.3	87.5	88.7	89.5	89.1	89.8	90.8	88.5	88.4				
5	Y	41	#12	92.6	92.8	93.2	92.2	88.0	88.0	88.3	87.0	92.2	91.2	92.2	91.8	89.6	88.8	90.6	89.7	91.1	91.4	88.7	89.0	91.8			
5	Y	171	#11	88.5	88.5	90.4	89.9	86.5	87.5	86.6	86.0	89.4	89.2	88.7	88.8	87.9	86.7	90.1	89.8	88.7	88.4	86.8	87.1	88.3	89.3		
5	Y	171	#12	89.4	90.1	89.6	89.6	90.9	87.9	91.2	90.7	89.1	89.3	89.3	90.2	89.0	91.1	90.1	90.2	89.1	89.6	89.6	89.5	89.3	89.2	87.2	

Figure S2

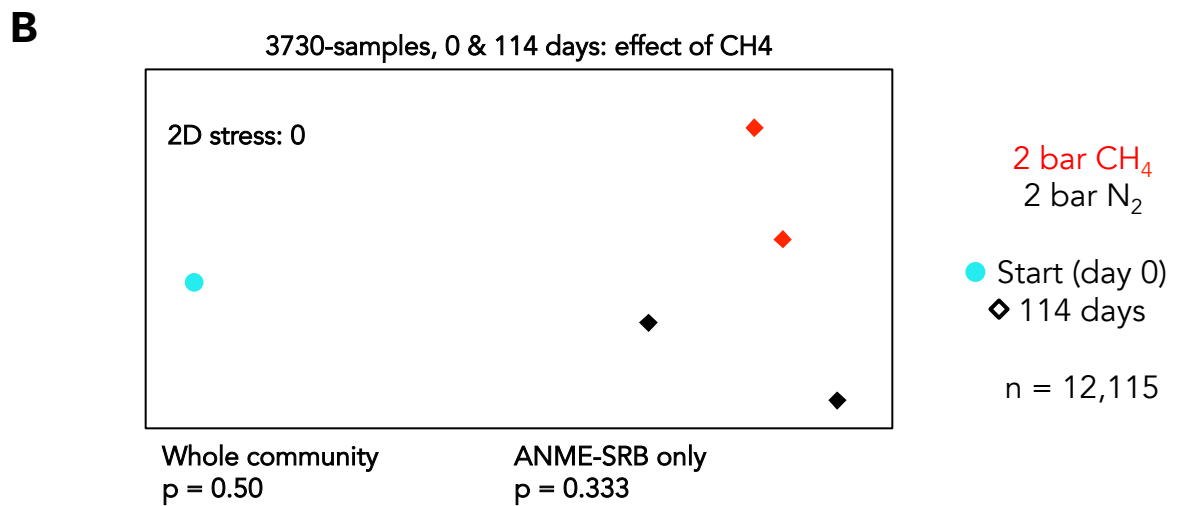
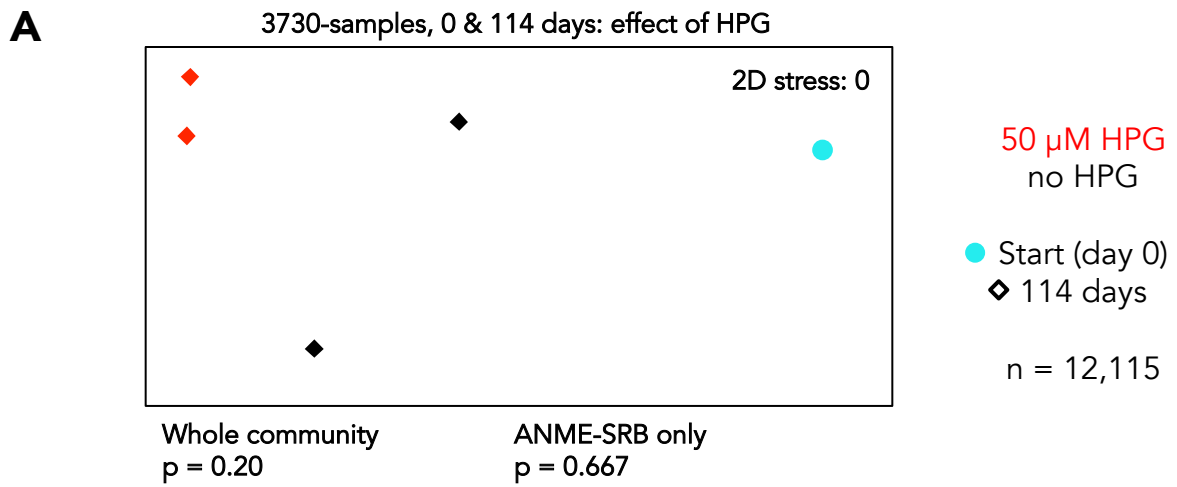
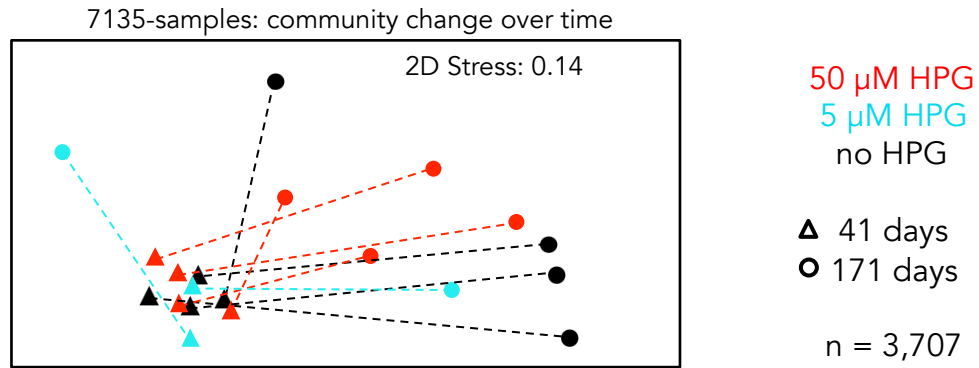
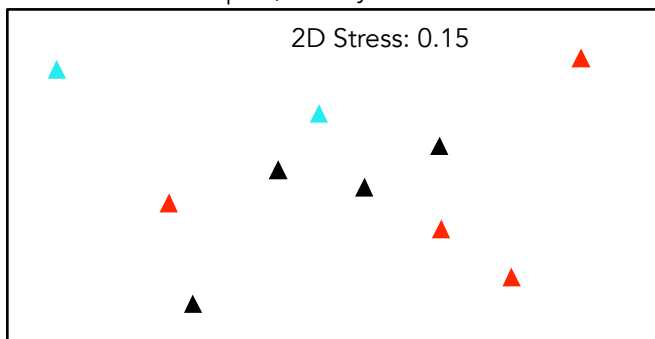


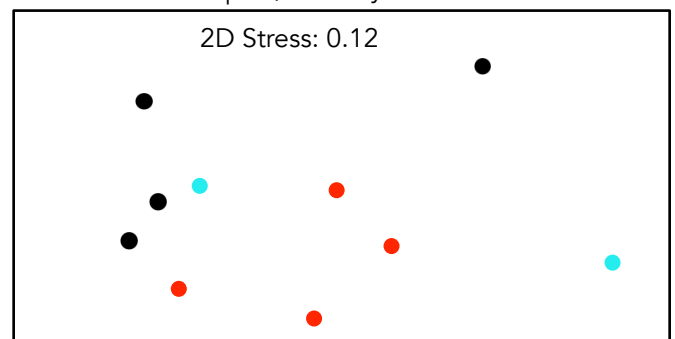
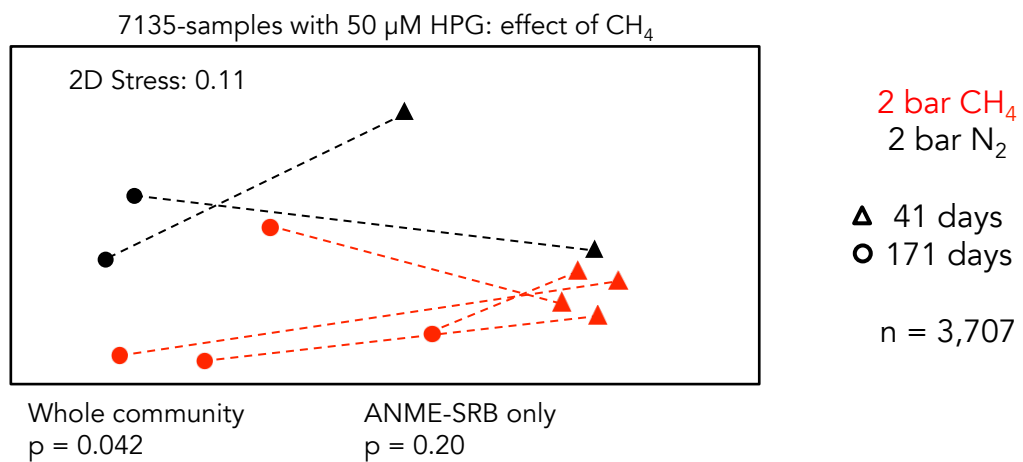
Figure S3

A

7135-samples, 41 days: effect of HPG

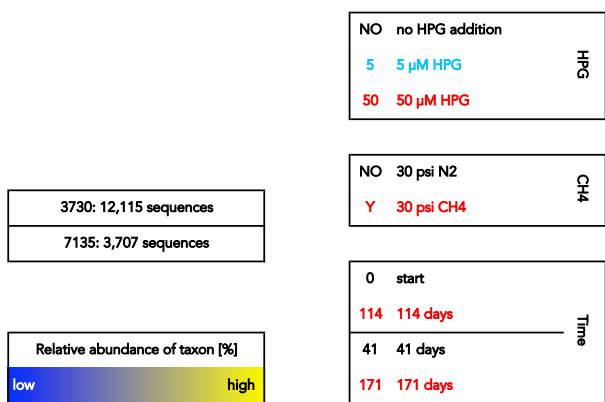


7135-samples, 171 days: effect of HPG

**B****Figure S4**

A

3730	HPG	NO	NO	NO	50	50	50	50
	CH4	Y	Y	Y	Y	Y	NO	NO
	TIME	0	114	114	114	114	114	114
	Sample	#0	#1	#2	#3	#4	#5	#6
ANME-1;Other		0.7	0.3	0.4	0.4	0.4	0.2	0.3
ANME-1;ANME-1a		20.3	14.6	15.0	12.8	15.7	9.8	12.4
ANME-1;ANME-1b		1.3	1.2	1.5	1.5	0.9	1.0	0.9
Methanosarcinales;ANME-2a-2b		9.7	6.0	7.9	6.1	5.2	4.5	6.5
Methanosarcinales;ANME-2c		6.1	5.8	5.0	6.9	7.0	4.2	5.6
Methanosarcinales;Methanosaetaceae		0.0	0.0	0.0	0.1	0.0	0.0	0.0
Desulfarcales;Desulfarculaceae		0.4	0.9	0.6	0.9	0.8	1.0	0.8
Desulfobacterales;Desulfobacteraceae		11.9	12.5	10.7	10.8	11.6	14.4	16.8
Desulfobacterales;Desulfobulbaceae		3.3	4.4	5.0	4.5	4.3	5.1	4.8
Desulfuromonadales;Desulfuromonadaceae		0.2	0.2	0.5	0.3	0.3	0.5	0.2
Other archaea		0.9	1.1	1.0	1.0	1.2	1.4	0.7
Other bacteria		45.1	52.9	52.3	54.7	52.6	58.0	50.9



B

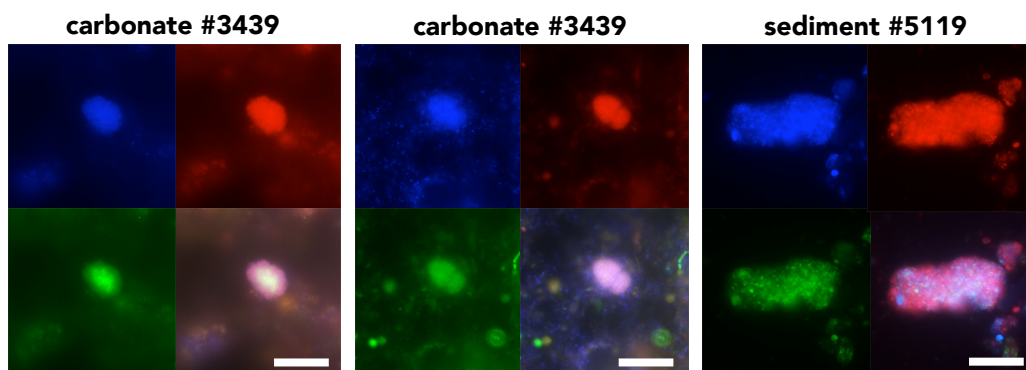
7135	HPG	NO	NO	NO	NO	NO	NO	NO	NO	50	50	50	50	50	50	50	50	50	50	50	50	50	50	50	50	50	50	50	50	50	50	50	50	50	50	50	
	CH4	Y	Y	Y	Y	Y	Y	Y	Y	Y	Y	Y	Y	Y	Y	Y	Y	Y	Y	Y	Y	Y	Y	Y	Y	Y	Y	Y	Y	Y	Y	Y	Y	Y	Y	Y	
	Time	41	41	41	41	171	171	171	171	41	41	41	41	171	171	171	171	41	41	171	171	41	41	171	171	41	41	171	171	41	41	171	171	41	41		
	Sample	#01	#02	#03	#04	#01	#02	#03	#04	#05	#06	#07	#08	#05	#06	#07	#08	#09	#10	#09	#10	#11	#12	#11	#12	#11	#12	#11	#12	#11	#12	#11	#12	#11	#12		
ANME-1;ANME-1a		2.3	1.7	1.9	4.2	3.2	1.3	2.1	5.4	3.3	2.8	3.4	1.8	3.3	2.1	1.5	3.6	0.7	1.6	1.5	1.2	1.2	1.9	2.6	2.4												
ANME-1;ANME-1b		0.3	0.2	0.3	0.2	0.1	0.0	0.1	0.1	0.3	0.1	0.2	0.1	0.1	0.0	0.1	0.1	0.1	0.1	0.1	0.2	0.2	0.1	0.2	0.2												
Methanomicrobia;D-C06;_f		0.0	0.0	0.0	0.0	0.0	0.0	0.0	0.0	0.0	0.0	0.0	0.2	0.0	0.1	0.0	0.0	0.0	0.1	0.0	0.0	1.1	0.0	0.0	0.1												
Methanosarcinales;ANME-2a-2b		0.7	0.7	0.9	0.7	1.3	0.5	1.5	1.0	0.4	0.8	0.5	0.9	0.6	1.4	0.8	0.5	0.3	0.2	0.3	0.4	0.7	0.5	0.7	1.1												
Methanosarcinales;ANME-2c		1.1	1.8	1.4	1.6	4.9	7.8	7.5	3.4	1.5	2.0	1.2	1.7	3.0	4.8	2.4	3.3	0.4	0.6	2.1	1.3	1.1	0.8	1.8	3.5												
Desulfarcales;Desulfarculaceae		1.1	0.9	1.0	0.9	0.8	1.0	0.9	0.9	1.0	1.1	0.8	0.9	0.9	1.0	1.2	1.2	1.5	1.0	0.9	1.2	0.9	1.1	2.0	0.9												
Desulfobacterales;Desulfobacteraceae		3.3	3.5	3.4	3.4	4.4	6.0	5.9	5.8	3.8	3.2	3.3	3.4	4.7	4.3	5.6	4.3	4.9	4.4	4.5	3.5	3.6	3.6	6.8	5.2												
Desulfobacterales;Desulfobulbaceae		3.2	2.8	2.8	2.8	2.8	2.6	2.3	2.3	2.5	3.0	3.3	2.6	2.2	3.0	2.9	2.9	2.4	3.3	2.1	2.0	2.6	2.6	3.2	2.9												
Other archaea		13.6	14.1	12.8	12.8	14.2	9.1	11.9	12.6	13.2	11.3	12.8	13.7	12.1	12.3	13.3	12.2	12.8	11.7	17.3	17.1	12.1	12.0	9.6	12.4												
Other bacteria		74.3	74.2	75.2	73.3	68.2	71.5	67.5	68.2	73.9	75.5	74.2	74.6	72.8	70.8	72.0	71.7	76.6	76.7	71.1	72.8	76.2	77.3	73.1	71.3												

Figure S5

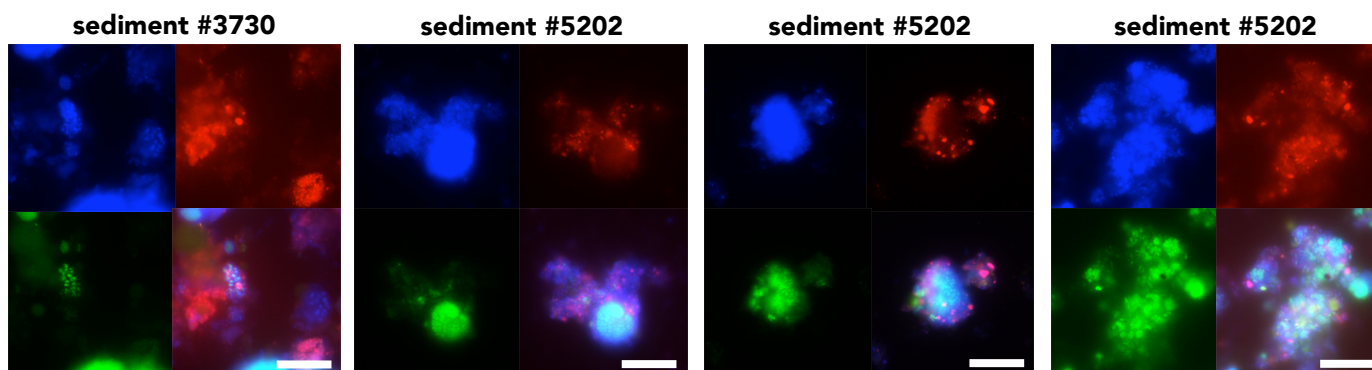
Figure S6



A DAPI (DNA) FISH (Arch915) FISH (EUB338-III+comp) Overlay Bar, 10 μ m



B DAPI (DNA) FISH (Arch915) FISH (Ver47+helper) Overlay Bar, 10 μ m



C DAPI (DNA) BONCAT FISH (Arch915) FISH (EUB388-III) Bar, 10 μ m

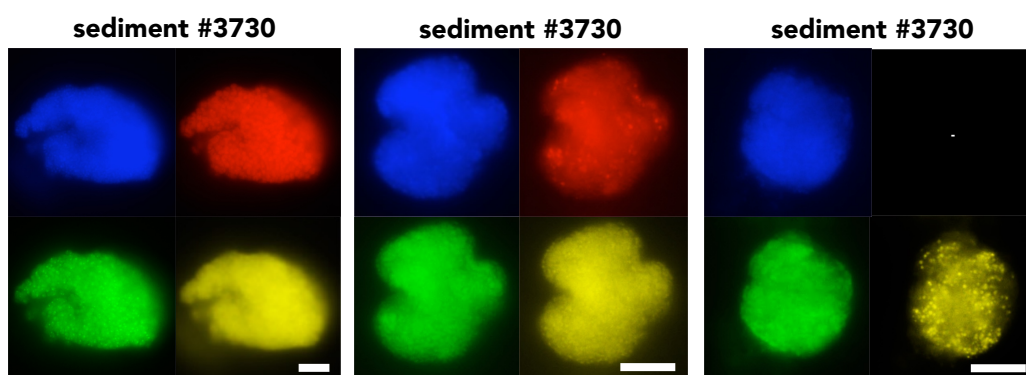


Figure S7